6. SITE 114

The Shipboard Scientific Party[1]
With Additional Reports From
F. Aumento and B. D. Clarke, Dalhousie University, Halifax, Nova Scotia,
and
J. R. Cann, University of East Anglia, Norwich, United Kingdom

Location: Sediment discontinuity at anomaly 5 on east flank of Reykjanes Ridge.

Position: 59° 56′N, 26° 48′W, (celestial navigation).

Depth of water: 1927 meters (corrected).

Total penetration: 623 meters.

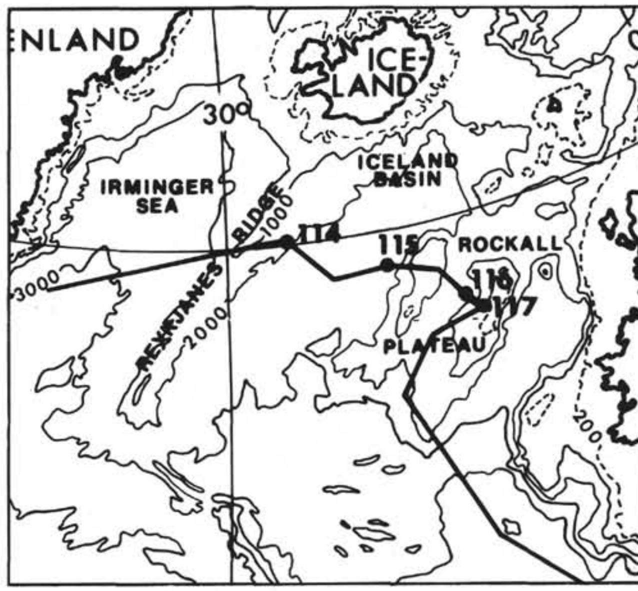

SITE BACKGROUND AND OBJECTIVES

The site was chosen to obtain data about the evolution by sea floor spreading of the Reykjanes Ridge and hence of the north Atlantic. The Reykjanes Ridge runs southwest from Iceland and is part of the mid-Atlantic Ridge system. Its shape was first investigated in detail by Ulrich (1960) during cruises of V. F. S. *Gauss* and F. F. S. *Anton Dohrn* in 1957 and 1958. To the northeast it joins the Reykjanes Peninsula in Iceland, and to the southwest it runs straight as far as 55°N where it is offset to the east by a series of fracture zones, the principle one of which is the Gibbs (or Charlie or 53°N) Fracture Zone.

Magnetic surveys have been made from the air by Canada (Godby, Hood and Bower, 1968) and by USNOO in cooperation with the Lamont Geological Observatory in 1963 (Heirtzler, Le Pichon and Baron, 1966). These revealed the striking linearity and symmetry of the magnetic anomalies associated with a spreading seafloor, and gave a spreading rate of 1 cm/yr for each limb. A comprehensive geophysical survey was made of the ridge in 1966 in R. V. *Vema* Cruise 23 during which the magnetic anomaly field was studied in greater detail; topography, sediment thickness, heat flow and gravity studies were made, and the crustal structure determined by seismic refraction (Talwani, Windisch and Langseth, 1971). Subsequently USNOO has made a detailed shipborne magnetic and bathymetric survey of part of the ridge and its flanks especially on the southeastern side (Johnson and Schneider, 1969; Avery, Vogt and Higgs, 1969). Dredging, coring, bottom photography and heat flow measurements have been made from R. V. *Trident* in 1967 by Krause and Schilling (1969) and de Boer, Schilling and Krause (1969, 1970).

Seismic reflection profiles (Talwani *et al.*, 1971) obtained on *Vema*-23 (Figures 1 and 2) have shown the distribution of sediment on the Reykjames Ridge. The central 40 kilometers of the ridge are almost completely free of sediments. The sediment thickness increases patchily up to 0.3 second away from the axis up to Magnetic Anomaly 5 (10 million years) where a basement scarp separates the inner and outer flank regions of the ridge. On the southeast side of the ridge beyond the scarp, sediment thicknesses of nearly 1 second are found. Further still to the southeast, the basement deepens beneath sediments reaching 1.5 to

[1] Anthony S. Laughton, National Institute of Oceanography, United Kingdom; William A. Berggren, Woods Hole Oceanographic Institution, Woods Hole, Massachusetts; Richard Benson, Augustana College, Rock Island, Illinois; Thomas A. Davies, Scripps Institution of Oceanography, La Jolla, California; Ulrich Franz, Technische Hochschule, Munchen, W. Germany; Lillian Musich, Scripps Institution of Oceanography, La Jolla, California; Katharina Perch-Nielsen, University Institute for Historical Geology and Paleontology, Copenhagen, Denmark; Alan Ruffman, Bedford Institute, Dartmouth, Nova Scotia (Present address: Seascope Consultants, Box 15-6-52, Purcell's Cove, Nova Scotia); Jan E. van Hinte, Imperial Oil Enterprises, Ltd., Calgary, Alberta; Robert B. Whitmarsh, National Institute of Oceanography, United Kingdom.

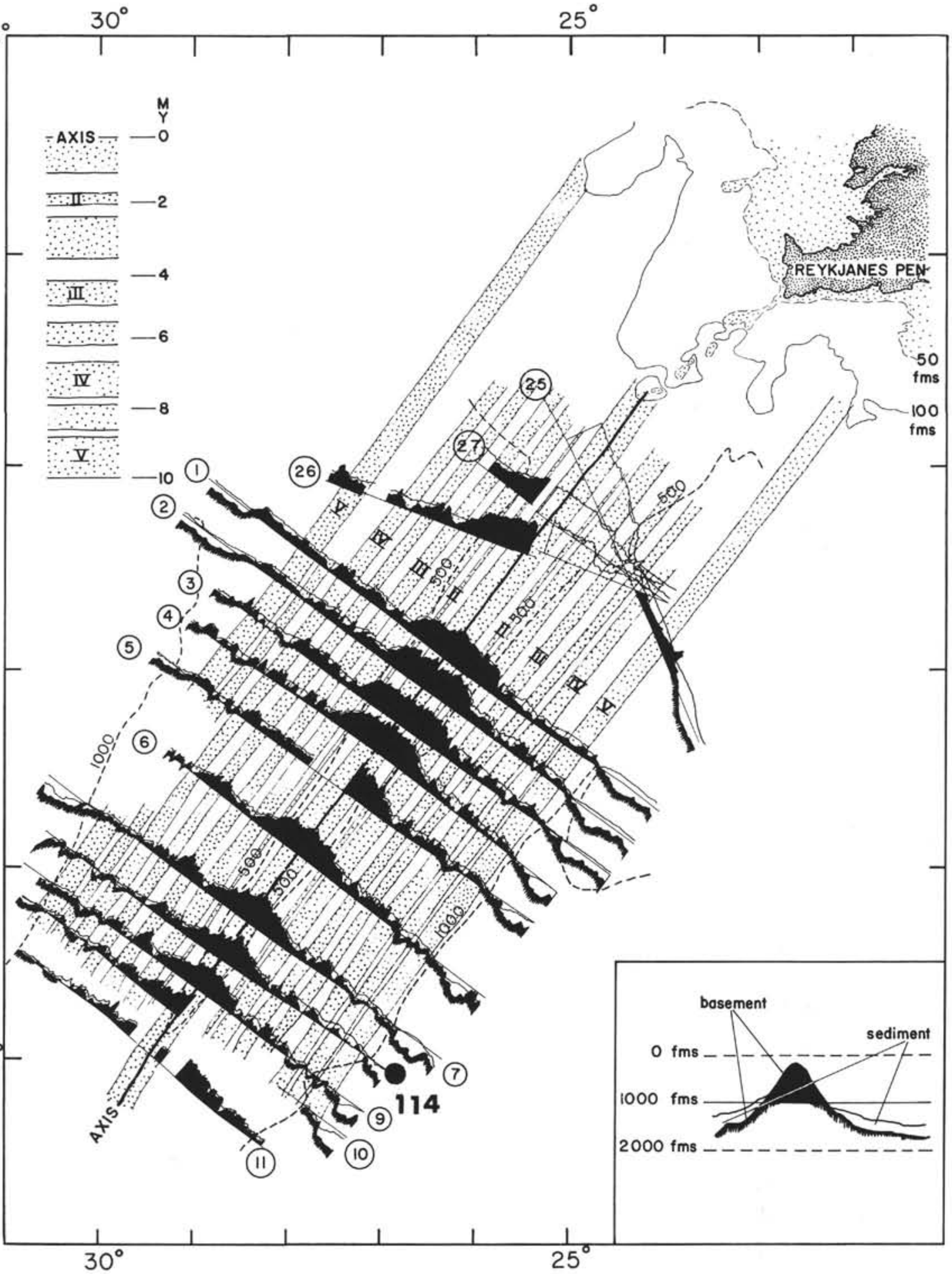

Figure 1. *Bathymetric and seismic reflection profiles across the Reykjanes Ridge superimposed on magnetic anomaly pattern (stippled) (Talwani, Windisch and Langseth, 1971).*

2.0 seconds thick. A broad rise in the sediments half way between the axis of the Reykjanes Ridge and Rockall Plateau has been mapped over a length of 700 kilometers and has been named the Gardar Ridge (Johnson and Schneider, 1969; Jones, Ewing, Ewing and Eittreim, 1970). It is believed to be due to sediment deposition from the east flank of a bottom current running southwest from the Norwegian Sea.

The sediment discontinuity associated with the basement scarp between the inner and outer flanks is remarkably parallel to the magnetic anomaly pattern. Similar discontinuities in sediment thickness have been reported from other cross sections of mid-ocean ridges and have been explained by a hiatus in sea floor spreading (Ewing and Ewing, 1967). Under conditions of a constant supply of pelagic sediments, the sediment thickness would

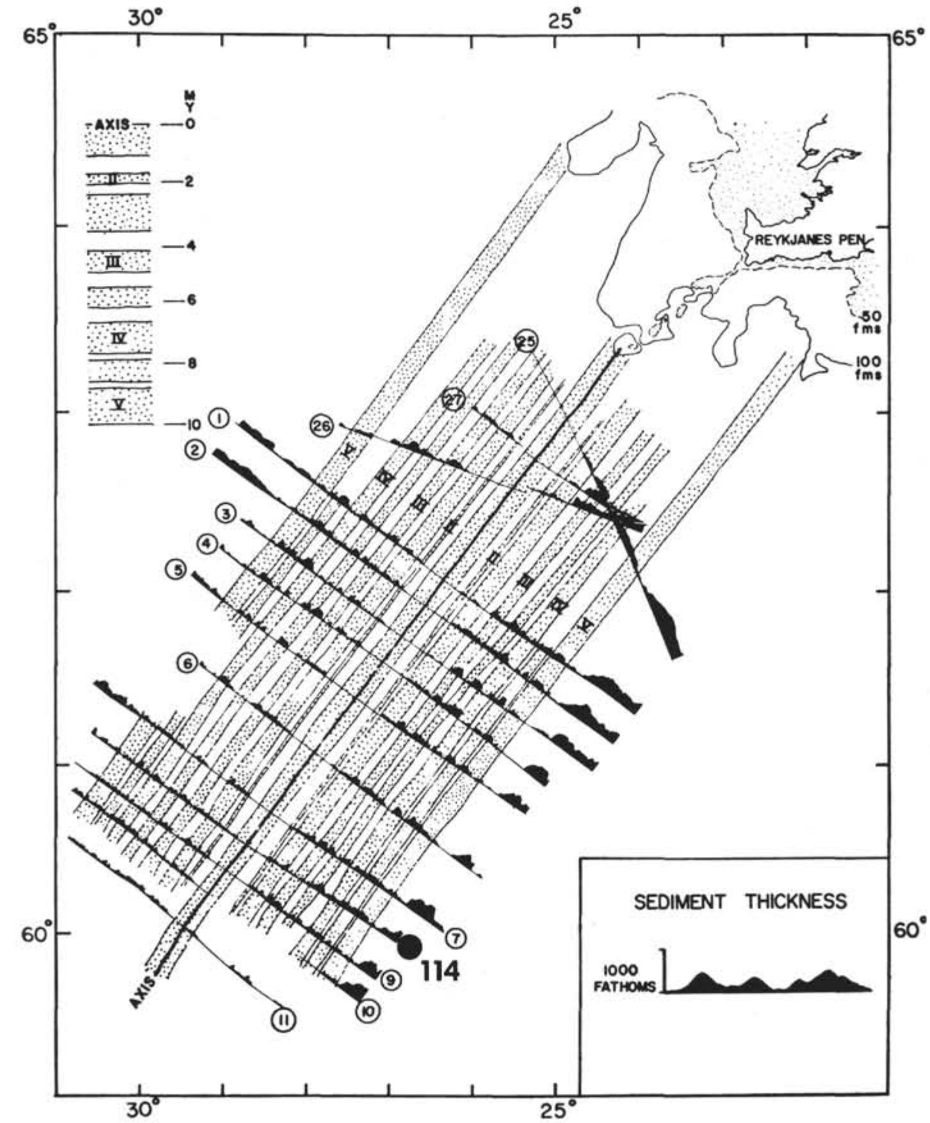

Figure 2. *Sediment thickness profiles on the Reykjanes Ridge, superimposed on magnetic anomaly pattern (Talwani, Windisch and Langseth, 1970).*

be proportional to the age of the crust beneath. Ewing and Ewing proposed a hiatus from late Mesozoic or early Tertiary up until about 10 million years ago when a new spreading cycle commenced. According to such a hypothesis, the oldest sediments immediately southeast of the sediment discontinuity on the Reykjanes Ridge should be 50 to 70 million years old in contrast to 10 million years immediately northwest of the discontinuity. Talwani *et al.* (1971) support the hypothesis of a hiatus or extreme deceleration in spreading rate to explain the sediment discontinuity, although they also suggest that the sediment distribution is strongly influenced by bottom currents. Pitman and Talwani (in press) have interpreted widely spaced magnetic profiles of the North Atlantic between the Azores-Gibraltar Ridge and the Gibbs Fracture Zone in terms of geochronology and conclude that between Anomaly 13 (38 million years) and Anomaly 5 (9 million years), the spreading rate fell to a very low value or that there may even have been a hiatus. Evidence for the extrapolation of this to the Reykjanes Ridge is not strong.

On the other hand, data from DSDP Leg 3 in the South Atlantic show that spreading was fairly uniform throughout the Cenozoic in spite of the sediment discontinuity described there by Ewing and Ewing (1967). Furthermore, the detailed magnetic surveys of USNOO on the Reykjanes Ridge have been interpreted by Vogt, Ostenso and Johnson (1970) in a manner inconsistent with the hiatus hypothesis. Between the axis of the ridge and Rockall Plateau, three zones of anomalies have been recognized.

The first zone against the west side of Rockall Plateau is characterized by well-developed linear anomalies trending 045°. These can be identified as Anomalies 24 (60 million years) to 15 (40 million years), and the spreading rate calculated parallel to the Gibbs Fracture Zone (095°) decreases from 1.7 cm/yr to 0.7 cm/yr. Between anomaly 5 and 18 (10-45 my) the lineation trend is 015°-025° and is broken by fracture zones every 100 kilometers. The spreading rate is 0.7-0.8 cm/yr in direction 095°. In the third and central zone, the anomalies trend parallel to the Reykjanes Ridge axis (035°) and again are continuous. The spreading rate in direction 095° is 1.13 cm/ yr. In the first and third zones, the magnetic anomalies make an angle of 30 to 40 degrees with the normal to the spreading direction. Vogt *et al.* (1969) relate these changes of trend and rate to changes in the position of the pole of rotation between the Greenland and northwestern European tectonic plates. The juxtaposition of Anomaly 24 with the west edge of Rockall Plateau defines the date of initiation of the separation at 60 million years ago.

On this interpretation, the sediment discontinuity occurs on the boundary of the two inner zones where the spreading rate increases from 0.8 cm/yr to 1.13 cm/yr. This change of rate would be scarcely perceptible in measurements of sediment thickness even under uniform sedimentation conditions. An alternative explanation must therefore be sought based on non-uniform sedimentation.

Site 114 was chosen to test these opposing explanations. Two holes were planned, one on either side of the discontinuity, in order to compare the ages of the oldest sediments and thus of the basement. Of the two, the critical hole was the one in the thick sediments on the older side where a basement age of 50 million years would be expected on the Ewing and Ewing theory, and 12 million years on the Vogt *et al.* theory. Therefore, this hole was drilled first and, subsequently, it proved unnecessary to drill the second.

An entirely different objective was to obtain some knowledge of the biostratigraphic column typical of a northern ocean area. Most previous DSDP holes had been drilled in equatorial or temperate zones and much of the Cenozoic biostratigraphy had been related to descriptions from these areas. New data was expected from high latitude (60°N) drilling where the water circulation depended on the proximity of the Arctic regions.

In summary, the objectives were:

(a) To date the oldest sediments above basement either side of the sediment discontinuity, in order to test the hiatus theory of seafloor spreading.

(b) To determine the nature of the thick sediment body and to determine the mechanism of deposition.

(c) To find and date the base of glacial derived sediments, and to establish the typical deep sea faunal assemblages at these northern latitudes.

SURVEY DATA

The sites for the two holes were chosen on the basis of an E-W *Vema*-23 crossing of the sediment discontinuity at 60°08′N. However, a failure in the satellite navigator three days before arrival at site and a continually overcast sky lead to considerable doubt about where we were. Subsequent fixes on site showed us to be 11 miles from the intended position.

For two reasons, it was decided to drill the southeast site before the northwest one. First, the navigational problem required that we find and cross Magnetic Anomaly 5 and the sediment discontinuity with the seismic profiler. Second, we believed that if the thick sediments could be explained by an abnormally high sedimentation rate, there would be no need to drill the northwest site.

After finding what appeared to be the thick sediment sequence starting at 1130 hours on July 11, some doubt was raised by subsequent thinning and faulting. At 1214 hours we altered the course to southeast at right angles to the ridge trend and steamed for another 10 miles before retracing our track at 5 knots to a suitable site (Figure 3). We were searching for a region where the basement was relatively well defined and the sediments had their maximum thickness so as not to miss the older section. Such a place was hard to find since the basement relief was about 800 meters and reflections from the valleys were poor. In the event, we found that we were successful in drilling into a valley.

The regional setting of Site 114 is summarized in Figure 3. The topography (modified from data by USNOO) clearly shows the NE-SW scarp separating the inner and outer flanks. Five *Vema*-23 and one *Glomar Challenger*-12 seismic profiles cross the sediment discontinuity within 80 kilometers of the site (Figures 4 and 5). A composite line drawing of a profile across the site is shown in Figure 6. The valley at the base of the scarp defines the northwestern edge of the thick sediment sequence, and its southeastern edge is less well defined near the 1200 fathom contour. The sediment sequence extends at least 300 kilometers parallel to the Reykjanes Ridge (Figure 2), but within the area of Figure 3 it is shown that it sometimes divides into branches running N-S. The cross section of the sediment ridge is sometimes domed, sometimes peaked, and it is piled much higher than the basement ridges which in no way act as barriers confining sediment ponding. The contact with the scarp is usually dipping toward the scarp and is often very sharp (Figure 4). Within the sediment the profiles show internal reflectors with wavy surfaces bearing no relation to basement relief. Some of these reflectors show peaks similar to the present day sea bottom and meet the basement at a downward dipping angle. This pattern, we believe, relates to a migrating ridge crest of sediments deposited from bottom contour currents.

The crests of positive magnetic anomalies are shown in Figure 2, Anomaly 5 being dated as 9.5 million years by Heirtzler *et al.* (1968). By linear extrapolation of a spreading rate of 1.0 cm/yr perpendicular to the ridge axis, the age of basement under Site 114 should be 12.0 million years.

After completion of drilling we steamed five miles northwest while streaming gear before making a slow traverse across the beacon. However, the weather conditions prevented us from maintaining contact with the beacon, and on the southeast track at 4.5 knots, we picked the beacon signal up when it was nearly abeam. We therefore traversed the site on a southwesterly course at 3.5 knots for three miles before resuming a southeasterly course for five miles at 4.5 knots.

Beneath Site 114 (Figure 7), three principal internal reflectors were seen at 0.19, 0.28 and 0.60 seconds. Basement was hard to see on the run across the beacon but was thought to lie at about 0.75 second. Basaltic basement was in fact drilled at 618 meters giving a mean velocity from sea bed to basement of 1.65 km/sec.

DRILLING OPERATIONS

Drilling operations started at 1545 hours on 11 July after the beacon had been dropped in 1927 meters of

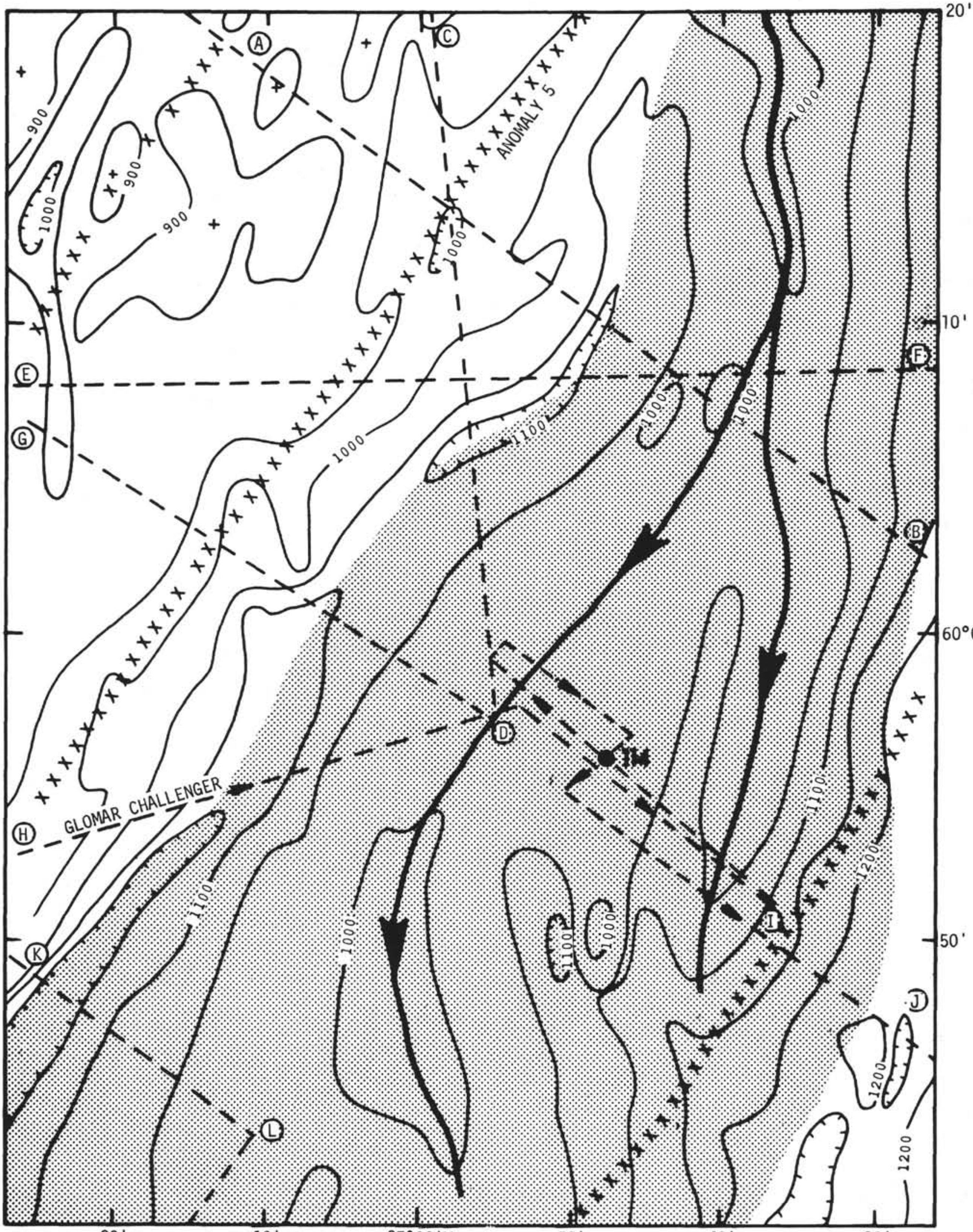

Figure 3. *Bathymetry in the vicinity of Site 114, showing location of thick sediment body (stippled), sediment ridge crest and inferred current direction (heavy arrowed line), tracks with seismic reflection profiles, (illustrated in Figures 5, 6 and 7) and the axes of positive magnetic anomalies (crosses).*

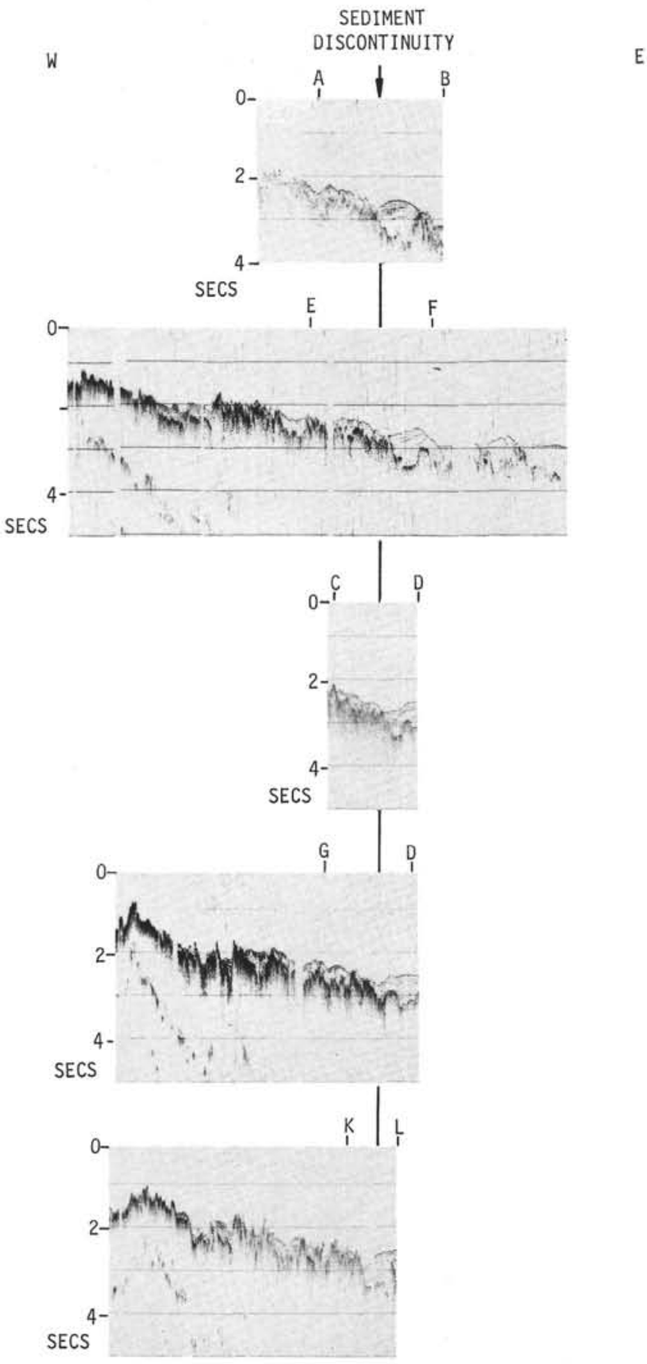

Figure 4. *Seismic reflection profiles by* Vema-*23 across the sediment discontinuity near Site 114. Positions are shown in Figure 3. The records illustrated are:*
Vema-*23, 1130-0830, 2 Sept. (Records 204-203)*
Vema-*23, 0700-2030, 22 Aug. (Records 145-149)*
Vema-*23, 2100-2330, 6 Sept. (Records 235-326)*
Vema-*23, 0630, 7 Sept. - 2330, 6 Sept. (Records 236-235)*
Vema-*23, 1800, 7 Sept. - 0230, 8 Sept. (Records 242-244)*
(by courtesy of Lamont-Doherty Geological Observatory)

water. The bottom hole assembly consisted of a Smith 4-cone tungsten carbide insert bit beneath 8 drill collars and 3 bumper-subs.

No attempt was made to feel bottom and drilling proceeded quickly with little weight to the first core at 100 meters. Regularly spaced cores of 100 meters were taken to 600 meters, the drilling being very easy throughout although considerable heave and roll due to bad weather made coring operations difficult. In many cases the liners had sections filled with water or slurried clay and this was probably due to lifting the bit off the bottom while coring. Even at 600 meters drilling went abnormally easy and the 600-meter core was recovered within 18 hours of entering the bottom. Throughout, the sediments were gray silty clays.

While drilling beyond 609 meters, a very hard layer was encountered at 618 meters and so a core was cut. However a nominal 9-meter cut gave only a shattered core catcher and a few grains of basaltic sand that showed we were drilling basement. Another core obtained one cobble of basalt and the final core between 622 and 623 meters cut a 30-centimeter core of basalt. While cutting basement the heave was such that the bumper-subs were being fully extended and collapsed, a movement of 5 meters, and hence the drill bit occasionally pounded the bottom. In these circumstances it was extremely hard to feel bottom, and progress was by instinct.

The sediments had showed an abnormally high sedimentation rate, adequate to explain the sediment discontinuity by bottom current action. It was not expected to be possible, in the light of the material recovered, to define the onset of glaciation or the Pliocene-Pleistocene boundary, so no more coring was needed. The hole was therefore terminated at 0045 hours on July 13th, and we departed from site at 0800 hours. Out of 60 meters cored, 46 meters were recovered (77 per cent).

TABLE 1
Cores Cut at Site 114

Hole	Core	Core Interval (m, subbottom)	Core Recovered (m)
114	1	100-109	7.75
114	2	200-209	9.25
114	3	300-309	4.70
114	4	400-409	9.28
114	5	500-509	9.25
114	6	600-609	5.20
114	7	618-621	Fragments only
114	8	621-622	Few cobbles only
114	9	622-623	.30

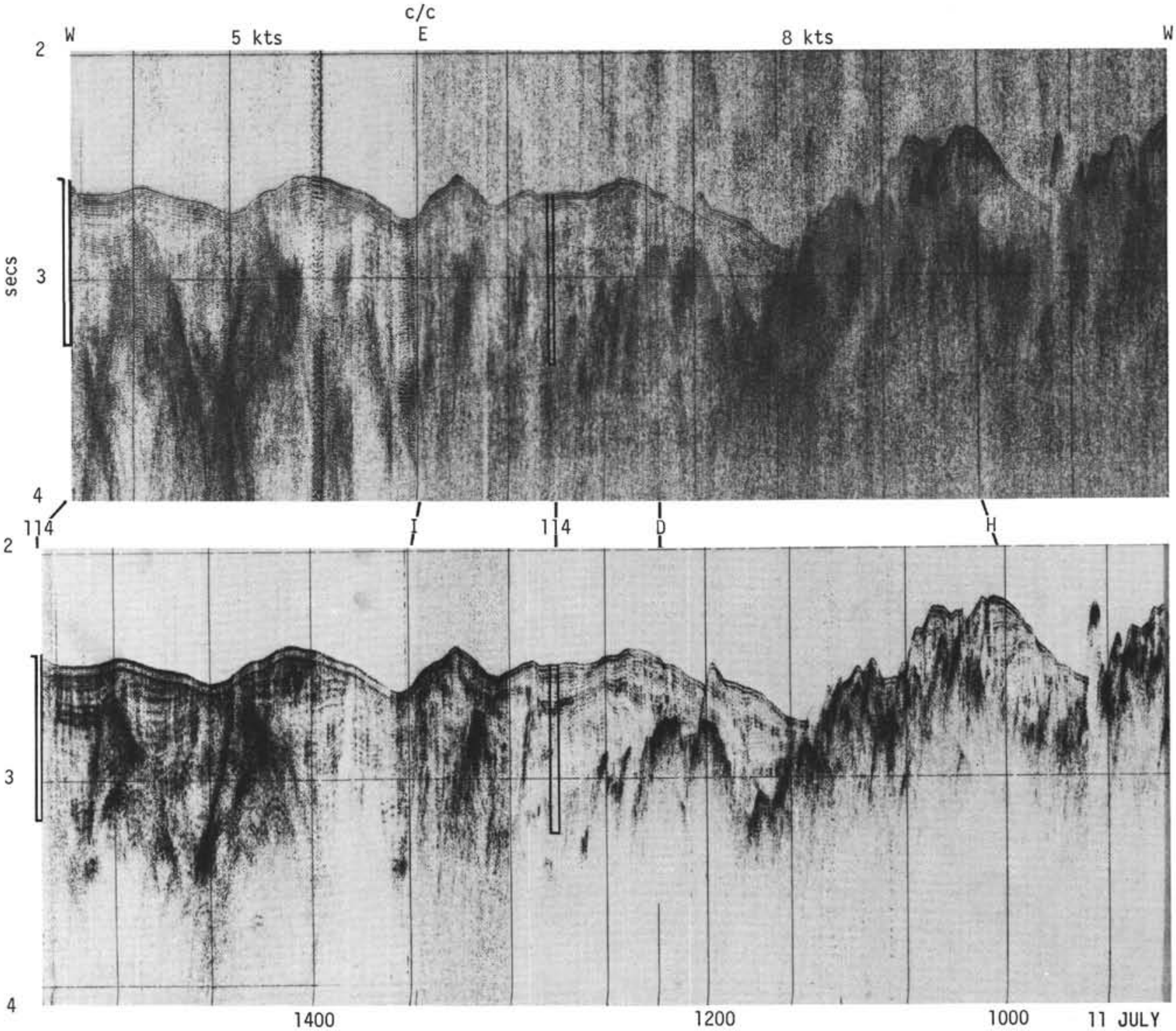

Figure 5. *Seismic reflection profile by* Glomar Challenger *on approach to Site 114. See Figure 3 for track. Upper record filtered at 80-160Hz, lower record at 160-320 Hz.*

LITHOLOGY

The sediments cored at Site 114, on the eastern flank of the Reykjanes Ridge, consist entirely of clayey silts with, in a few places, sandy horizons. Basalt was cored at the bottom of the hole.

Preliminary Report on the Petrography of the Basalt

F. Aumento and B. D. Clarke, Dalhousie University, Halifax, Nova Scotia, and J. R. Cann, University of East Anglia, Norwich, United Kingdom

Sample 114-8-CC

This is a very fine-grained, almost aphyric basalt, perhaps a devitrified basalt glass. The rare phenocrysts are of olivine replaced by iddingsite and plagioclase. The groundmass is very fine-grained and rather oxidized, containing relics of clinopyroxene, plagioclase and skeletal iddingsitized olivine. Vesicles are partly or completely filled with carbonate, chlorite and zeolites.

Samples 114-9-1, 0-4 cm, 17 cm and 22-30 cm

All three samples are of almost aphyric variolitic basalt. The rare phenocrysts are of olivine (sometimes fresh, but often replaced by iddingsite and carbonate), and fresh clinopyroxene. The groundmass consists of skeletal plagioclase microlites and small grains of clinopyroxene set in a dark, devitrified, cryptocrystalline matrix which is highly oxidized. Vesicles are filled with chloritic material.

From sample 114-9-1, 22 to 30 centimeters, P. J. Ryall reports abundant partly maghemitized Class 1 titanomagnetite; his results are:

Trace element analyses have yielded the following results (in ppm).

Ti	Rb	Sr	Y	Zr	Nb
6400	3.5	75	24	49	3.0

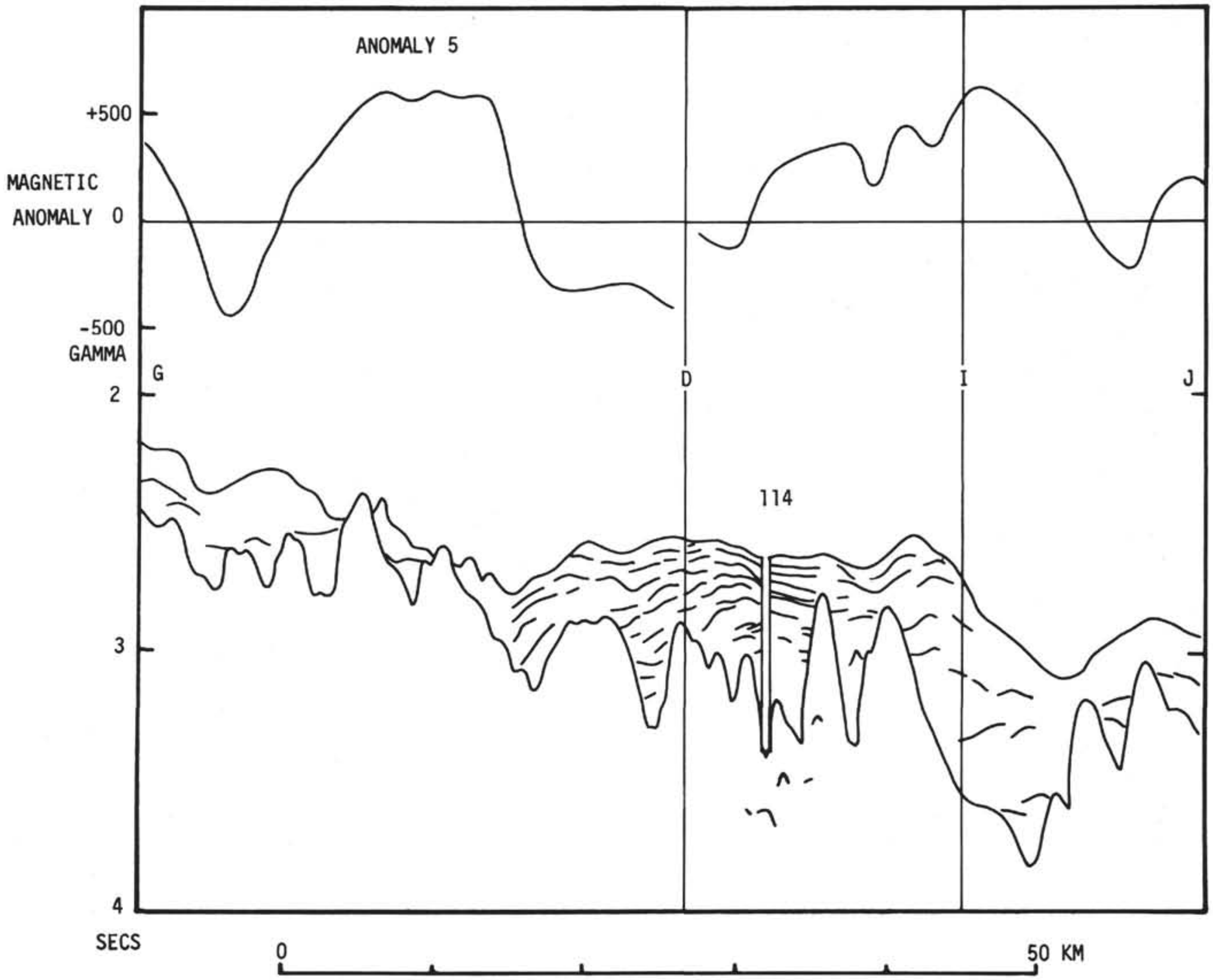

Figure 6. *An interpreted seismic profile across Site 114 constructed from* Vema-*23 and* Glomar Challenger-*12 data, with magnetic anomaly profile.*

Sample 114-9-CC

This is a clear, pale yellow isotropic basalt glass, with dark banded devitrification centers nucleated on microphenocrysts. Euhedral olivine phenocrysts are surrounded by perlitic cracks. This glass would be suitable for fission track dating if more pieces were available.

Discussion

All of the samples from this hole are of very rapidly chilled, subaqueously extruded basalt, almost completely free of phenocrysts. Petrographically they strongly resemble other ocean floor basalts, though again the presence of clinopyroxene phenocrysts is an unusual feature. Thus they appear on these grounds to represent oceanic volcanic basement lying beneath the sediments. They are somewhat weathered, though rather less so than the basalts from Hole 112, and could be estimated to be several million years old. Although they are not suitable for potassium-argon dating, the glass of the catcher sample of Core 9 would, if more were available, be very suitable for fission track dating.

The Sediments

All the sediment cores taken at this site are very much disturbed, especially the lower ones. This is probably due to the appreciable movement of the ship causing the drill bit to lift off the bottom and, thus, initiating a pumping action while coring. In those parts of the cores which are believed to be comparatively undisturbed, very little structure could be seen. In some places there was a suggestion of faint lamination and in Core 6 some crossbedding and slump structures could be seen, but there is no sign of graded bedding. Burrow mottling is not common in the upper part of the section cored, but some mottling was visible in Cores 5 and 6 and occasional worm burrows were found throughout the cores. The absence of burrowing and the few structures seen suggest that the material cored was deposited comparatively rapidly with perhaps an increasing sedimentation rate above Core 5.

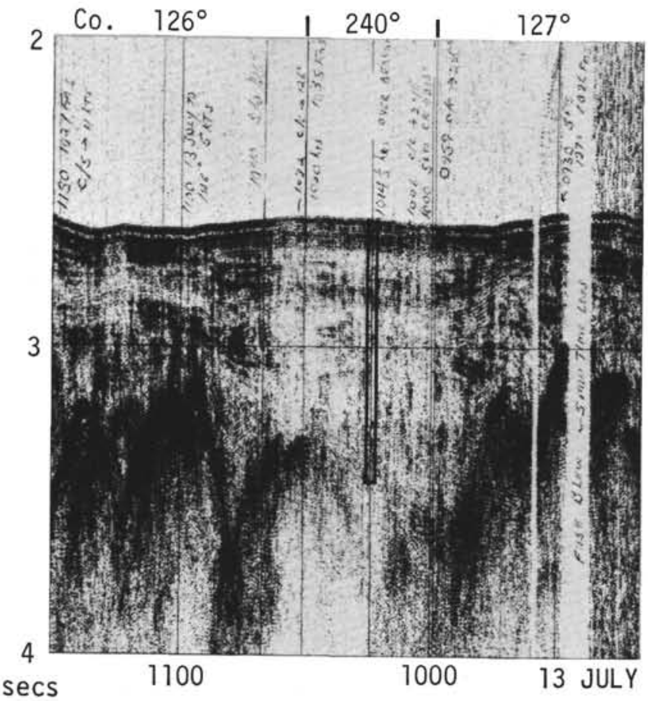

Figure 7. *Seismic reflection profile across beacon after drilling.*

In texture, the sediments are all clayey silts, (Appendix B and Figure 8) in some places indurated enough to be called soft mudstones. Some layers rich in foraminiferal sand occur in Core 2 and a few pebbles (? ice-rafted) appear in Cores 1 and 2. The carbonate content of the sediments is generally low, less than 20 per cent (Appendix C), although markedly higher in the upper part of Core 5. In Figure 2 the carbonate content of the samples has been plotted against the percentage of sand-sized material. The line in Figure 9 represents the function: per cent carbonate = per cent sand. This, of course, would be the situation if all of the carbonate was found in the sand fraction and all of the sand fraction was in fact carbonate. The apparently linear relationship between carbonate content and grain size suggests that the bulk of the sand fraction is indeed composed of foraminifera. All of the points are displaced above the line, however, because of the presence of coccoliths in the silt and clay size fractions which contribute to the overall carbonate content.

Compositionally, the sediments are essentially uniform; a fact which in itself–since these are clearly not deep sea pelagic oozes–suggests rapid accumulation. Because of erosion the supply of terrigenous material tends to change in composition with time. If the sedimentation rate were low, we would consequently expect to see variations in the composition of the sediments deposited through more than half a kilometer of section. Appendix A shows the composition of the smear slides examined. The coarse fraction obtained during grain-size analysis was also examined and shows a composition essentially the same as that seen in the smear slides. Volcanic glass, mica flakes, palagonite, chlorite, zeolites, pyrite, "glauconite", rare quartz and feldspar, diatoms, sponge spicules and nannofossils occur throughout the sequence. The volcanic glass is of several varieties, both colorless and colored in various shades of brown. Fresh chips of glass and highly altered fragments quite commonly appear together suggesting that glasses from different sources or of different vintages have been deposited together. Palagonite (altered glass) is common in the middle part of the sequence (Cores 3, 4 and 5). Both chlorite and zeolites (phillipsite, etc.) occur commonly in all the cores, but chlorite is noticeably more abundant in the upper part of the sequence (Cores 2, 3 and 4), whereas, zeolites are more common in the lower part (Cores 4, 5 and 6). Small grains of pyrite were seen in all samples, and several pyrite nodules (up to 1.5 centimeters across) were found in Core 3. Pyritized worm tubes were found in Core 4, and in Core 5 many of the foraminifera are either cemented by pyrite or have pyrite crystals growing either in or on them. A second iron mineral, orange red in transmitted light, probably limonite or goethite occurs sparsely in all sections. It appears to be an alteration product of "glauconite" for in some slides small green grains of "glauconite" can be seen changing to the orange mineral at the edges and corners. "Glauconite" both as irregular grains and as replaced foraminifera occurs in all sections, but is markedly less abundant in Cores 3 and 4 than in the upper and lower parts of the sequence. Quartz and feldspar are not common and detrital minerals seem to be absent.

Radioloria, diatoms and sponge spicules are quite common. In some samples these are so abundant that the sediment could almost be described as a siliceous ooze. Foraminifera are moderately common except in Core 4 where they are rare. They frequently appear as "glauconite" moulds. Mollusc shell fragments were seen in several cores.

The interpretation of the sedimentary succession is not entirely clear. The rapid rate of accumulation, the abundant silt-sized particles and the few structures seen suggest transport and deposition by fairly strong bottom currents; but the good state of preservation of the diatoms and the fragile "glauconite" moulds of foraminifera (assuming they were formed prior to deposition at the present locality) suggest the opposite. The shell fragments may suggest

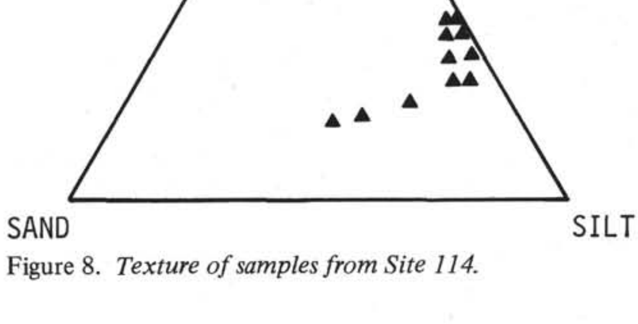

Figure 8. *Texture of samples from Site 114.*

material from deeper water. There seems to be no contribution to the sediments from land other than volcanic material.

Clearly these are not typical calm water deep-sea oozes, nor are they turbidite deposits, so characteristics of abyssal plains. It is possible that these are the type of deposits which we might expect if, as has been suggested on the basis of the seismic reflection profiles, the thick pile of sediments in this region is the result of bottom currents flowing south along the eastern flank of the Reykjanes Ridge, although there is no positive indication, from the nature of the sediments alone that this has been the case. Such currents, while moderately strong, would be gentle enough to transport planktonic material, such as diatoms, and maybe even small "glauconitized" foraminifera, without significant abrasion. They would also transport any material, such as shell fragments, which might find its way over a shelf edge into deeper water. Further, the rapid accumulation of sediment and the abundance of volcanic glass would ensure that within the sediments there was a chemically active environment in which alteration and solution of carbonate and probably further "glauconitization" could proceed. Without a better knowledge of the chemical relationships of the various minerals seen and the physical-chemical conditions under a contour current, these interpretations must be somewhat speculative.

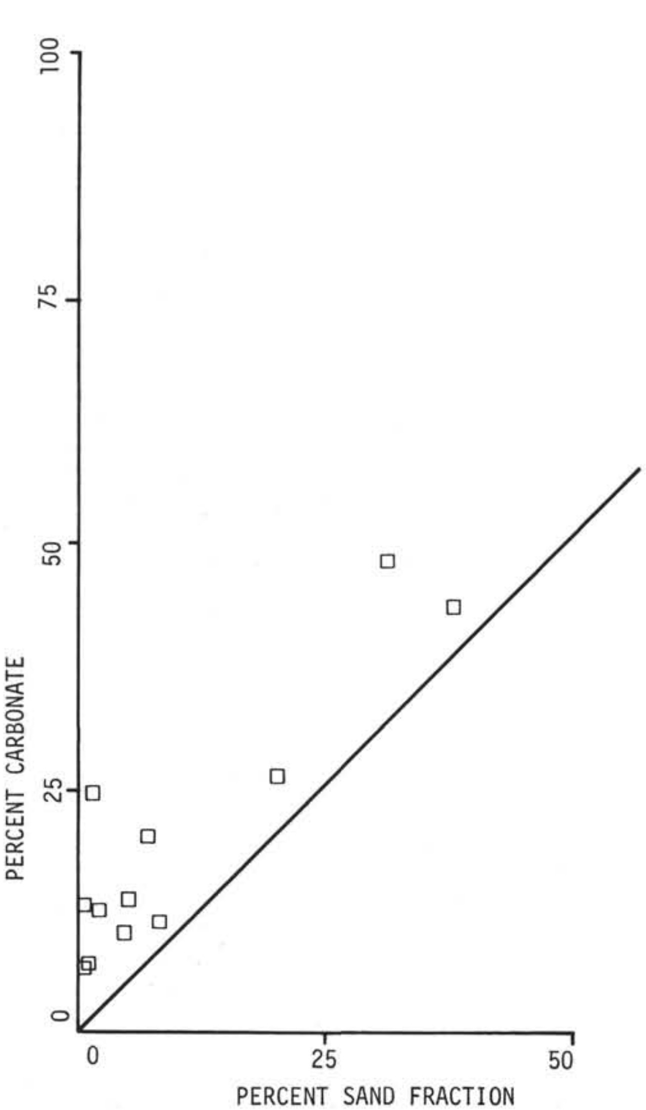

Figure 9. *Relation between carbonate content and sand fraction for samples from Site 114.*

PHYSICAL PROPERTIES

Measurements were made on six cores spaced at one hundred meter intervals. Due to considerable ship motion during coring many of the cores are very watery especially the whole of the following sections 114-3-2, 114-3-4, 114-4-2 to 114-4-6 and 114-5-1 to 114-5-4. In drawing the trend lines on the density, impedance, porosity and gamma plots allowance has been made for such watery cores.

Density and velocity increase slightly but systematically with depth from 1.45 to 1.7 gm/cc and from 1.5 to 1.6 km/sec, respectively, over the interval 100 to 600 meters. Sediment firmness similarly increases slightly with depth. The slight but uniform increase of these properties reflects the unvarying lithology of the sediments cored. Similarly the gamma activity is very uniform and close to 700 counts in the unwatery cores. This value is rather low considering the common occurrence of glauconite(?) and phillipsite and that most of the 16 carbonate samples from this site gave values between 10 and 25 per cent, but is possibly due to the high content of nonradioactive organic silica in many of the cores. The basalt recovered in Section 114-9-1 had the unusually high velocity of 5.89 km/sec.

Paleomagnetic measurements were conducted by J. Ade-Hall on a single oriented basalt sample from 114-9-1, 22 to 30 centimeters. There is a strong horizontal component of magnetization in this specimen so that the detection of apparently reversed magnetization in the rock is an uncertain result.

Depth of Reflectors

Of the four reflectors identified on the air-gun records at 0.19, 0.28, 0.60 and at around 0.75 seconds only the latter can be correlated with cored material. The deepest reflector is clearly the basaltic basement found at 618 meters. These data are summarized in Figure 10.

PALEONTOLOGY AND BIOSTRATIGRAPHY

General

The sediments are characterized by large quantities of diatoms and, in some instances, sponge spicules. Radiolarians are common to abundant in Cores 1, 3, 4 and 5. Evidence of glauconitization and silicification of calcareous microfossils can be seen, particularly in Core 5 (500 to 509 meters). The upper 500 meters represent Pliocene and Pleistocene (Figure 11); it is not possible to determine whether Core 6 (600 to 609 meters)—the oldest sediment core at this site—is of Miocene or Pliocene age. Basalt was cored 9 meters below the last sediment core (6), and it is probable that the oldest sediment above basement is of approximately the same age as Core 6. The Pliocene-Pleistocene boundary is drawn arbitrarily at 250 meters, midway between Cores 2 and 3. The Late Pliocene preglacial/

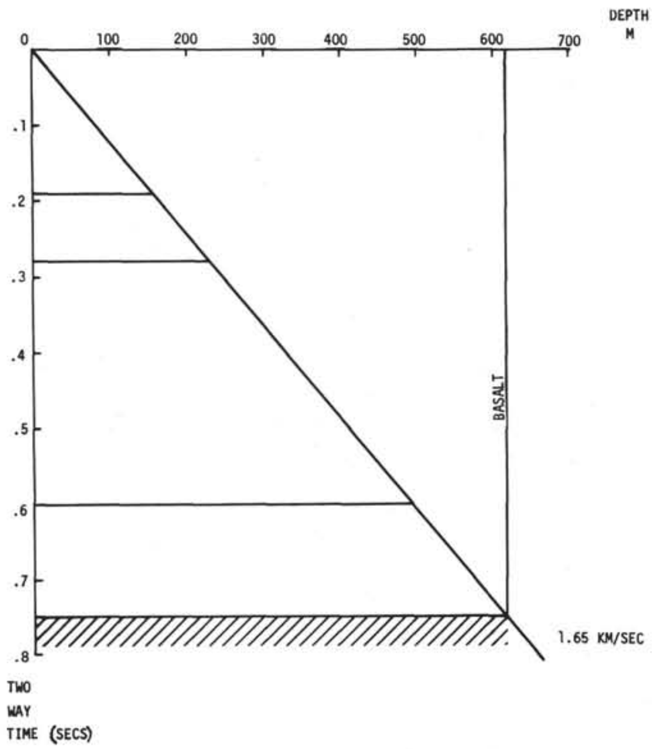

Figure 10. *Two-way travel times below the sea-bed of observed reflections plotted against the downhole depths of horizons believed to have given rise to these reflections. The mean velocity to the deepest reflection associated with a definite depth is given close to the line representing this velocity.*

glacial boundary is arbitrarily placed at 350 meters, midway between Cores 3 and 4.

Discussion

Foraminifera

Pleistocene

Cores 1 and 2 (100 and 200 meters) are of Pleistocene age. Planktonic foraminiferal fauna consist of *Globigerina pachyderma, Globigerina bulloides* and *Globorotalia inflata. Globorotalia crassaformis, G. scitula* and *Hastigerina siphonifera* occur in smaller numbers at some levels. The benthonic foraminiferal fauna, though generally sparse, contain such forms as *Planulina bradii, Hoeglundina elegans, Melonis pompilioides, Melonis barleeanum* and *Eponides tener*. The number of specimens as well as species diversity is markedly reduced below Core 1.

Pliocene

Cores 3 to 5 (300 to 500 meters) are of Pliocene age. In Core 3 (300 to 309 meters) the fauna is dominated by a robust four-chambered globigerinid, which is referred to here as *Globigerina atlantica*. This form appears to exhibit a marked degree of morphologic variability and may have been recorded under several different names in various papers dealing with Late Neogene biostratigraphy of the Mediterranean region. *Globorotalia inflata* occurs rarely with this form in Core 3. Core 4 (400 to 409 meters) contains a similar but still further numerically reduced fauna, consisting of *Globigerina atlantica, G. bulloides, Globorotalia scitula* and *Orbulina universa*. Core 5 (500 to 509 meters) is dominated by relatively large robust specimens of *Globigerina atlantica, G. bulloides* and *Globorotalia inflata*. Core 6 (600 to 609 meters) contains a fauna dominated by a four-chambered form in which the chambers are strongly appressed, the final chamber nearly closing the umbilical region. These specimens are also referred to *Globigerina atlantica*. Examination of water samples from Cores 7 and 8 failed to yield diagnostic species of foraminifera.

Volcanic glass shards, sponge spicules, and diatoms are common throughout this sequence, particularly in Cores 3 through 6. Core 5 is characterized almost throughout by the abundant occurrence of a green authigenic mineral resembling glauconite. It fills the interior of foraminiferal tests in many cases.

The monotonous planktonic foraminiferal fauna of Pliocene age, dominated by the presence of *Globigerina atlantica*, is similar to conditions observed at Sites 111, 112 and 113.

Calcareous Nannoplankton

? Late Miocene to Pliocene and Pleistocene coccolith assemblages were found in the sediments of Site 114.

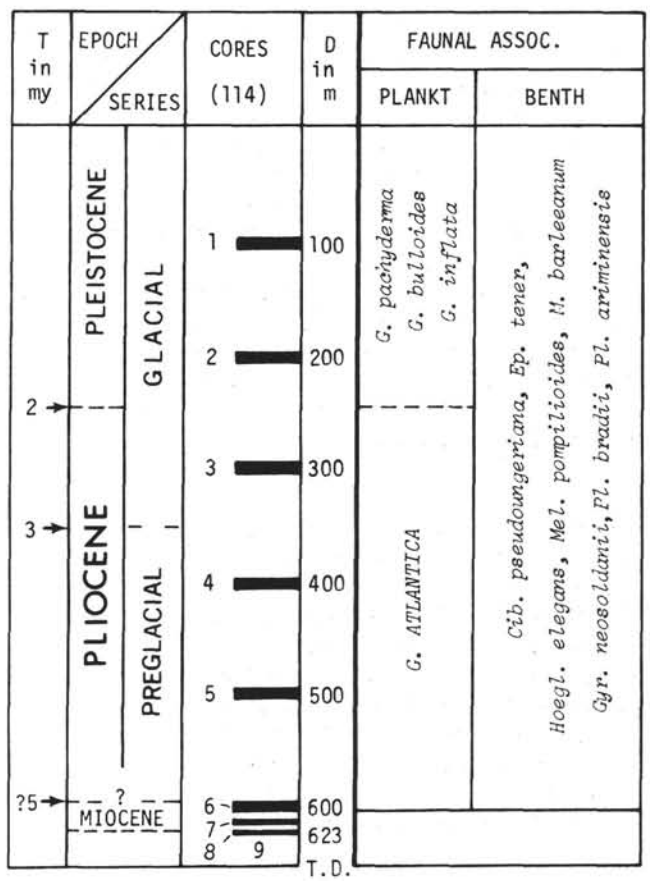

Figure 11. *Late Pliocene-Pleistocene foraminiferal faunal associations at Site 114.*

Pleistocene

Early Pleitocene coccolith assemblages were found to occur in Cores 1 and 2, here both assigned to the *Pseudoemiliania lacunosa* Zone. In Core 1, *Coccolithus pelagicus* is extremely rare, while it is abundant in Core 2, the same being true for *Helicopontosphaera sellii.* It has been shown that living *Coccolithus pelagicus* is absent in water temperatures of 7 to 14°C. Generally, the assemblages are still poor; *Syracosphaera, Rhabdosphaera clavigera* or *Cyclococcolithus macintyrei* occur only in a few samples. *Coccolithus pelagicus* in Core 2 includes again varieties with a small central opening and with a bar or a cross spanning the opening.

Pliocene (+ Miocene?)

Cores 3 to 8 contain Pliocene assemblages, and maybe also Miocene is present. In Core 3, discoasters are present, although rare. Also present is *Sphenolithus neoabies* and *Reticulofenestra pseudoumbilica* or a form similar to it. *Pseudoemiliania lacunosa* and *Cyclococcolithus macintyrei* are absent. In Core 4 the two latter species are sporadically present; in Sections 4 and 5, *Ceratolithus* sp. was found, but no sphenoliths occur in this core, which is assigned to the Late Pliocene, despite the lack of discoasters. In Core 5, discoasters are present again, but extremely rare. Here, *Reticulofenestra pseudoumbilica* is abundant and *Rhabdolithus* sp. is present throughout the core. In the top of Core 5, *Ceratolithus* sp. and *Scyphosphaera* sp. are present. They were also found in 5-5 and 5-6. The core can be assigned to the *R. pseudoumbilica* Zone or older, further zonation being impossible due to the lack of ceratoliths and more discoasters. Also Cores 6 and 7 show similar assemblages including occasionally *Sphenolithus abies, S. neoabies, Discoaster brouweri, D. variabilis* and *Rhabdolithus* sp. Here too, the assemblages lack age diagnostic forms to determine, whether Pliocene or Miocene is present.

The coccoliths found in the few marl pieces of the core catcher of Core 8 and in the water coming up with Core 7 are not age diagnostic, except for parts of a discoaster in Core 7 that seems related to *D. bollii*, a mid-Miocene form.

Generally the coccolith assemblages at Site 114 are poor, but many specimens are present. Again, the discoaster content is extremely small, a fact seen in the Pliocene at all other sites in high latitudes.

Radiolaria

Radiolarians are present in all cores from Hole 114, but they are particularly abundant in residues below the Pliocene-Pleistocene boundary in Cores 3, 4 and 5. Spumellarians dominate all assemblages both in terms of numbers of individuals (particularly of discoidal species) and species. Except for single specimens of *Stichocorys peregrina* (Riedel) in Cores 5 and 8, no other known age diagnostic fossils are present. Because of the high sedimentation rate at Site 114 (see below) only core catcher samples were examined, and these do not reveal any significant differences in assemblages from core to core.

Pleistocene

Theocalyptra davisiana (Ehrenberg) and species of discoidal spumellarians are the dominant radiolarians from Cores 1 and 2 of Pleistocene age. The former appears to be ubiquitous and often dominant in Pleistocene (and glacial Pliocene ?) assemblages from Leg 12 Sites in the North Atlantic.

The common radiolarians from Core 1 (about 50 species) are characterized by *T. davisiana, Actinomma* spp., *Spongopyle osculosa* Dreyer, *Spongotrochus* sp. cf. *S. glacialis* Popofsky, *Spongodiscus biconcavus* (Haeckel) Popfsky, and *Ommatodiscus* spp. Other less abundant species include *Druppatractus* sp. cf. *D. pyriformis* (Bailey), *Actinomma antarcticum* (Haeckel) (also present in Cores 2 and 3), *A. medianum* Nigrini (also present in Cores 2, 3, 6 and 8), *Stylodictya validispina* Joergensen, *Haliodiscus asteriscus* Haeckel, *Peripyramis circumtexta* Haeckel, *Cornutella profunda* Ehrenberg, *Micromelissa* sp., *Spongocure puella* Haeckel, *Phorticium pylonium* (Haeckel ?) Cleve, *Artostrobium auritum* (Ehrenberg), *Euchitonia* sp., *Eucyrtidium* sp., *Siphocampe* sp., and *Dictyophimus gracilipes* Bailey. Most of the above species are illustrated and described by Benson (1966) from the Gulf of California.

Radiolarians are rare in Core 2. The 25 to 30 species are dominated by *Theocalyptra davisiana, Ommatodiscus* spp., and other spongodiscids.

Pliocene

Radiolarians are abundant to very abundant in the Pliocene section represented by Cores 3, 4 and 5. The assemblages are overwhelmingly dominated by discoidal spumellarians (as listed above) which are of rather large size compared to most radiolarian species (major diameters 200 to 400 microns). There is the possibility that the large numbers of these specimens at Site 114 are the result of size sorting by currents rather than high productivity in the overlying waters. This would not be inconsistent with the proposed explanation that the abrupt increase in sediment thickness east of Magnetic Anomaly 5 is the result of differential deposition by bottom contour currents.

Ommatodiscus sp. dominates the assemblage of about 30 to 35 species from Core 3. *Druppatractus irregularis* Popofsky is common and persists through Core 8 but occurs no higher than Core 3. *Theocalyptra davisiana* is rare and disappears below Core 4. The most characteristic feature, however, is the abundant but only occurrence in Hole 114 of specimens of *Spongaster* sp. cf. *S. tetras* Ehrenberg which differs from *S. tetras* Ehrenberg in not consisting of a quadrangular, spongy, discoidal structure with four mutually perpendicular, denser rays but, instead, four relatively narrow distinct rays, with or without a secondarily developed patagium (Chapter 16, Plate 1, C-E). This species also occurs in Core 1, Hole 116 and Core 8, Section 6, Hole 116A, in both instances at and just below the transition from preglacial Pliocene without ice-rafted detritus to glacial Pliocene with ice-rafted detritus. As discussed above the glacial-preglacial boundary is placed arbitrarily midway between Cores 3 and 4 of Hole 114; therefore, the above stratigraphic levels at Site 116 correlate fairly well with the single occurrence of this species in Core 3, Hole 114. The short term presence of this species perhaps represents a migration event which may have time-stratigraphic significance in this part of the north Atlantic.

Core 4 is dominated by *Ommatodiscus* spp. and *Spongodiscus biconcavus. Euchitonia* sp. is common. This core marks the first downhole occurrence of *Eucyrtidium calvertense* Martin.

Core 5 is characterized by the nearly complete dominance (about 70 percent) of the radiolarian assemblage by *Spongodiscus biconcavus*. Except for decreases in the abundances of *Ommatodiscus* sp. and *Euchitonia* sp. and a slight increase in *Stylodictya validispina*, the assemblages from Cores 4 and 5 are similar. Core 5 marks the first downhole occurrence of *Stichocorys peregrina* (Riedel 1) (one or two specimens).

Radiolarians are rare in samples from Cores 6 and 8. There are no significant faunal changes between the overlying Pliocene and the Pliocene-Miocene ? except that there is a reduction in numbers of the dominant discoidal species of Cores 3, 4 and 5. In Core 8 there is a slight increase in *Ommatodiscus* spp. and *Spongodiscus biconcavus.*

ESTIMATED RATES OF SEDIMENTATION

As in the case of Site 113, the basis for the calculation of the rates of sedimentation is poor. An attempt, however, has been made to calculate them for general comparison. The result is shown in Figure 12.

The Pliocene-Pleistocene boundary is drawn arbitrarily at 250 meters, midway between Cores 2 and 3 on paleontologic data. The Late Pliocene preglacial/glacial boundary is arbitrarily placed at 350 meters, midway between Cores 3 and 4, also on paleontologic data. This yields an estimated average rate of sedimentation of about 12 cm/1000 yrs for the three million years of the Late Pliocene-Pleistocene at Site 114.

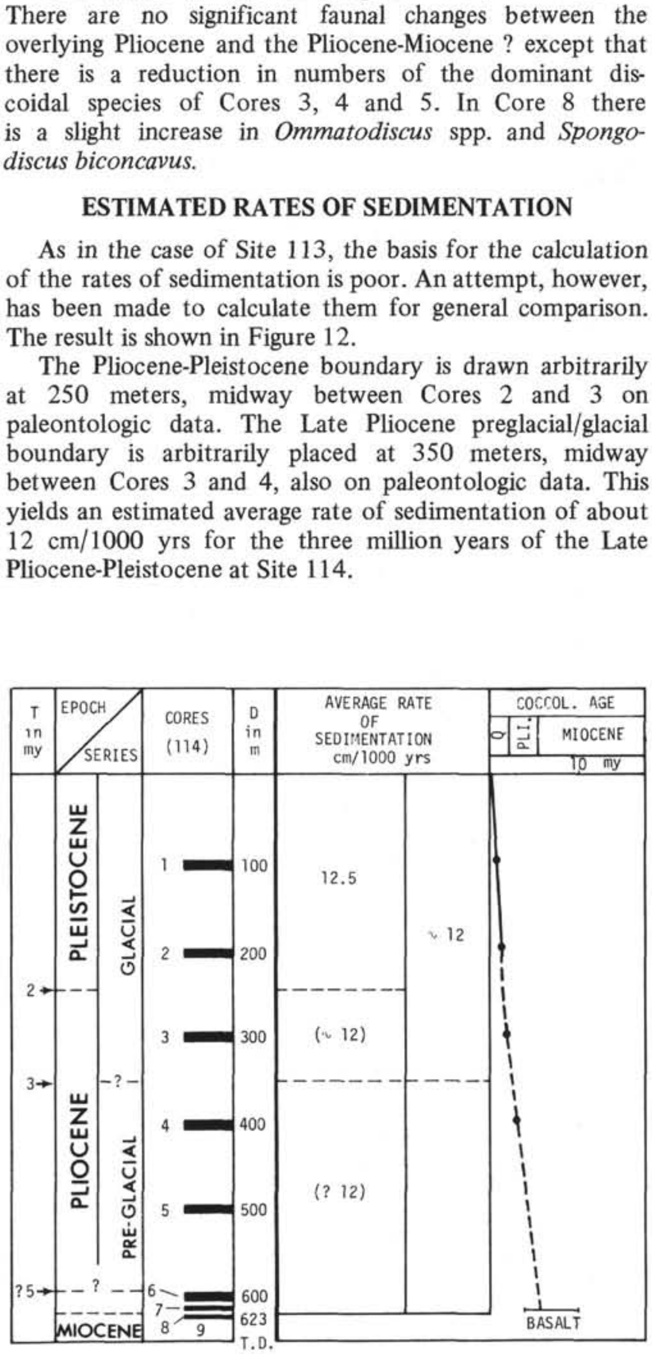

Figure 12. *Estimated average rates of sedimentation at Site 114.*

Downward extrapolation of the same sedimentation rate would suggest that the Miocene/Pliocene boundary (=5 million years) is at about 600 meters (at the top of Core 6). This is shown questionable in Figure 10, as there is no paleontologic data to allow a precise age determination of Core 6.

It would appear that the sedimentation rate was more or less continuously high and may not have been significantly affected by glaciation. Sediment composition (volcanic detritus) and texture (clayey silts) suggest that the relatively high sedimentation rate is due primarily to rapid accumulation of volcanic particles and siliceous and calcareous microplankton by deep flowing currents.

The uniform lithology and increase of density with depth allow the sedimentation rates to be corrected for natural consolidation. Using a density gradient of 0.00030 gm/cc/m, the sedimentation rate of 12 cm/1000 yrs becomes 14.6 cm/1000 yr.

DISCUSSION

Introduction

Site 114 was drilled to a total depth of 623 meters and bottomed in basalt. Nine cores were taken, the first six of which were at 100 meters intervals. Total core recovery was 45.7 meters out of 60 meters cored. The upper 500 meters represent Pliocene and Pleistocene. The sediments overlying basement at this site have been dated as Late Miocene–Early Pliocene. The sediments are essentially lithologically uniform—silty clays or sandy silts. The pelagic component forms a minor part of the total amount. Molluscan shell fragments have been found in several cores. These facts suggest that deposition in this region has been by fairly strong bottom currents. This explains the high rate of sedimentation (~12 cm/1000 yrs) for the Late Cenozoic sequence at this site.

The Age of the Basement Either Side of the Sediment Discontinuity

The main objective of drilling at this site was to determine whether there was evidence for a hiatus in sea floor spreading prior to Anomaly 5 (10 million years) which could account for the abrupt increase in sediment thickness east of the scarp associated with the anomaly. According to the hiatus theory of Ewing and Ewing (1967), a basement age of 50 million years would be expected below the site, whereas on a continuous spreading theory the age should be 12 million years.

The oldest sediments sampled in Hole 114 at a depth of 618 meters were Lower Pliocene, or possibly Miocene, giving a probable age of 5 my to the sediments within a few meters of basement. The seismic reflection profiles across the beacon (Figure 7) showed that the hole was drilled in a basement valley and that it is unlikely that sediments appreciably older than this existed in the vicinity. A fairly uniform sedimentation rate, corrected for consolidation, of 15 cm/1000 yrs is an order of magnitude higher than that typical of pelagic sedimentation. Moreover, the sedimentation rate clearly varies rapidly across an E-W section (Figure 6) since the beds are not uniformly draped over the topography. The basic underlying assumption of Ewing and Ewing, of uniform continuous sedimentation, is therefore not valid. The age of the oldest sediments is considerably younger than that required even of a continuous spreading theory and we therefore conclude that there is no evidence here of a hiatus in sea-floor spreading.

This conclusion from the results of Hole 114 made it unnecessary to drill another hole immediately west of the sediment discontinuity as originally proposed.

The Nature of the Sediment Body and the Mechanism of Deposition

Some important characteristic features of the sedimentation on the Reykjanes Ridge are shown by the seismic reflection profiles near Site 114:

(1) The sediment has accumulated in patches unrelated to the small scale basement topography.

(2) Internal layering shows no relation to the basement profile.

(3) The sediment body forms an elongated ridge parallel to the axis of the Reykjanes Ridge.

(4) The ridge crest has migrated westwards as the sediments have accumulated.

(5) There is a dipping contact between the sediment ridge and the basement scarp to the west.

(6) The ridge surface and the internal reflectors have a wavy surface (wavelength about 2 kilometers), the orientation of the wave crests being approximately parallel to the ridge.

These characteristics, as well as the lithological features discussed above, the apparent sorting by currents of the Radiolaria and the extremely high sedimentation rate, lead to the conclusion that the sediments have been deposited from a near-bottom current banked up against the Anomaly 5 scarp of the Reykjanes Ridge. Similar sediment ridges, the Gardar and Feni Ridges, have been deposited under the influence of bottom currents in the deeper Iceland Basin and in the Rockall Trough (Johnson and Schneider, 1969; Jones *et al.*, 1970).

Lee and Ellett (1965) have analyzed hydrographic sections across the North Atlantic and have identified the overflow of Norwegian Sea water across the Iceland-Faroe Ridge. One such section by R.R.S. *Discovery II* (Fuglister, 1960) crosses the Iceland Basin from the axis of the Reykjanes Ridge to Rockall Plateau near to Site 114 (Figure 13). Potential densities have been computed for this section and are shown in Figure 14. The horizontal density gradient implies a southward flow of water banked against the Reykjanes Ridge by Coriolis forces. By an analysis of salinity anomalies and of the dissolved oxygen content, Lee and Ellett traced the origin of the water to the Norwegian Sea. The section shows that the flow covers a depth range from 1200 to 3000 meters; in other words the whole eastern flank of the ridge is here subjected to bottom currents. Although the stations were separated by about 100 kilometers, there is some evidence that the flow is concentrated into narrower filaments, such as that between 2000 and 2200 meters below station 3842 immediately between the Gardar Ridge and Site 114 ridge.

A hydrographic section by *Erica Dan* in 1962 along 59°30'N across the Iceland Basin shows similar characteristics (Worthington and Wright, 1970), although at this time the bottom water flow did not appear to lap so high onto the Reykjanes Ridge. Worthington and Volkmann (1965) computed the volume transport across this section as 3.6×10^6 m^3/sec in a southwesterly direction and comment on the apparent irregularity of the flow. If the mean thickness of the flow was 200 meters over a width of 300 kilometers, the mean current would be 5 cm/sec (0.1 knots). However, it is unlikely that the flow is uniform over this front and if higher velocity filaments exist these may rise to 50 cm/sec (1 knot).

A composite seismic profile (Figure 14) from the axis of the Reykjanes Ridge to Rockall Plateau (from *Vema*-23, *Vema*-27 and *Discovery*-29 data) together with other seismic sections across the ridge (Talwani, Windisch and Langseth, 1971) and detailed bathymetric charts (Johnson and Schneider, 1969) show that the sediment is deposited irregularly in a series of ridges parallel to the Reykjanes Ridge, and hence parallel to the direction of bottom currents. Two such ridges are well mapped; that through Site 114 and the Gardar Ridge (Figure 13). However it is apparent from Figure 14, that other ridges probably exist. The question arises as to why the ridges are so well defined and why sedimentation has taken place over a period of many million years in one place and none in another. It is unlikely that higher velocity filaments of the bottom current could maintain position over this length of time without being controlled by the bottom topography. It is suggested therefore that the Norwegian Sea overflow water is divided into a series of streams (with, perhaps, slightly different potential densities and therefore in equilibrium with the topography at different depths), and that these are locally accelerated or decelerated by the actual topography encountered. Such topographic barriers as the scarp between the inner and outer flanks of the Reykjanes Ridge which extends some distance can guide the 2000-meter water and can control the balance between erosion or nondeposition in the higher velocity and turbulent part of the stream and deposition from the lower velocity parts, to build up the sediments sampled in Hole 114. In the same way, but on a larger scale the Gardar Ridge is banked against the buried basement scarp at about 3000 meters depth. At least two intermediate ridges are suggested by the seismic profile. A remarkable consequence of such a mechanism is that the Norwegian Sea water has flowed past this section in this way throughout the late Tertiary and that these sediments have been accumulating on the same ridges in spite of the gradual growth of the Reykjanes Ridge (and, hence, of the North Atlantic) and the vertical crustal movements associated with it.

The absence of sediments older than 5 million years on oceanic crust "dated" by magnetic anomalies to be 12 million years shows that little sediment was received during the first 7 million years of the life of this piece of basement. This is somewhat surprising in view of the sediment accumulations in valleys of the ridge now younger than 7 million years (Figure 14). It suggests that during the period 5 to 12 million years ago, the ridge crest may have either have been shallower than the present crest, and hence not washed by the Norwegian Sea overflow, or that the currents were strong enough to prevent appreciable deposition.

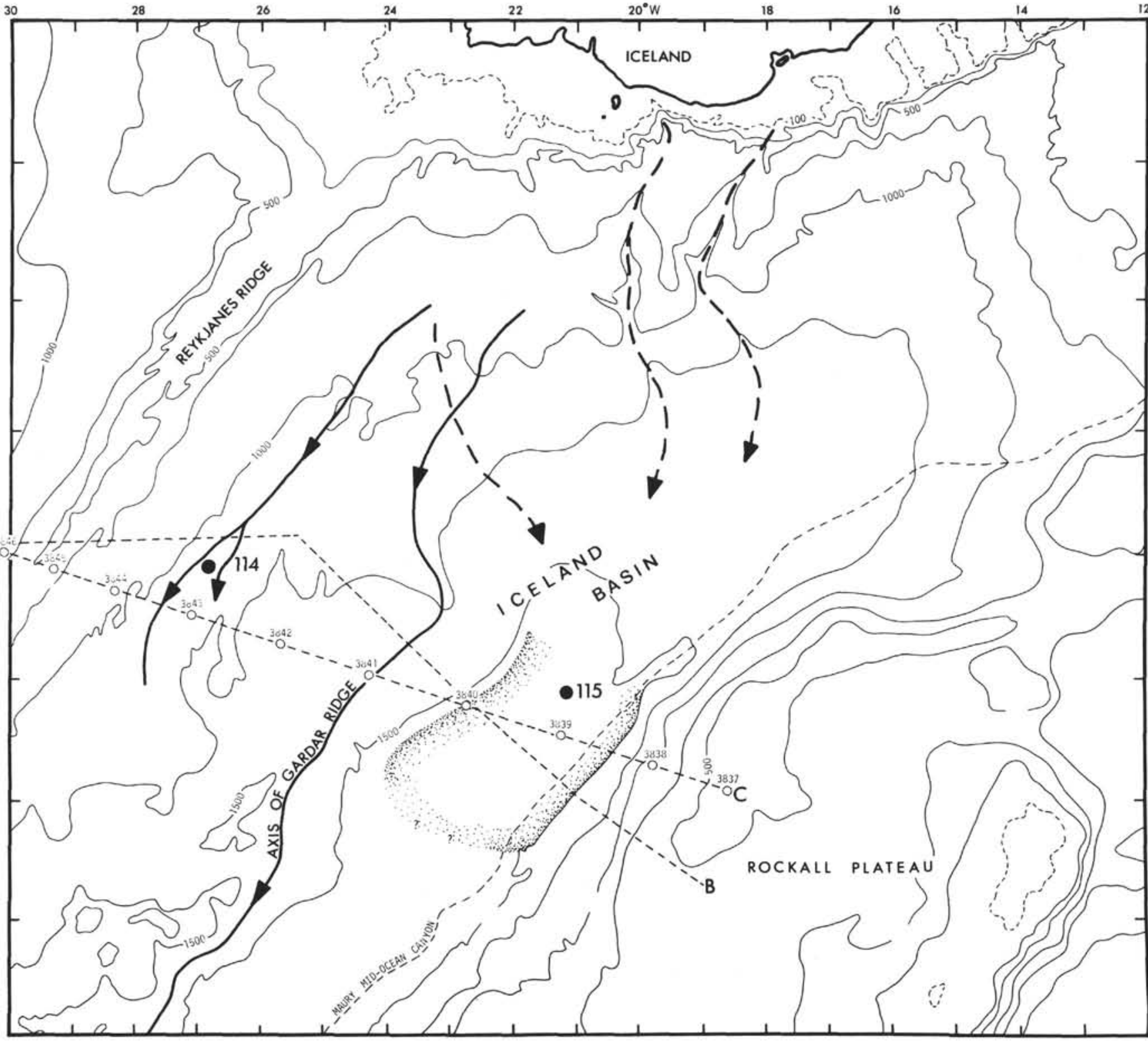

Figure 13. *Bathymetry of the Iceland Basin (depths in uncorrected fathoms 800 fms/sec) showing axes of 114 and Gardar Ridges (heavy arrowed lines), paths of turbidity currents (dashed arrowed lines), area of ponded turbidites near Site 115 (stippled). Seismic reflection profile AB is illustrated in Figure 14b. The results of hydrographic stations 3837-3846 (*Discovery-II*) on line A C are shown in Figure 14a.*

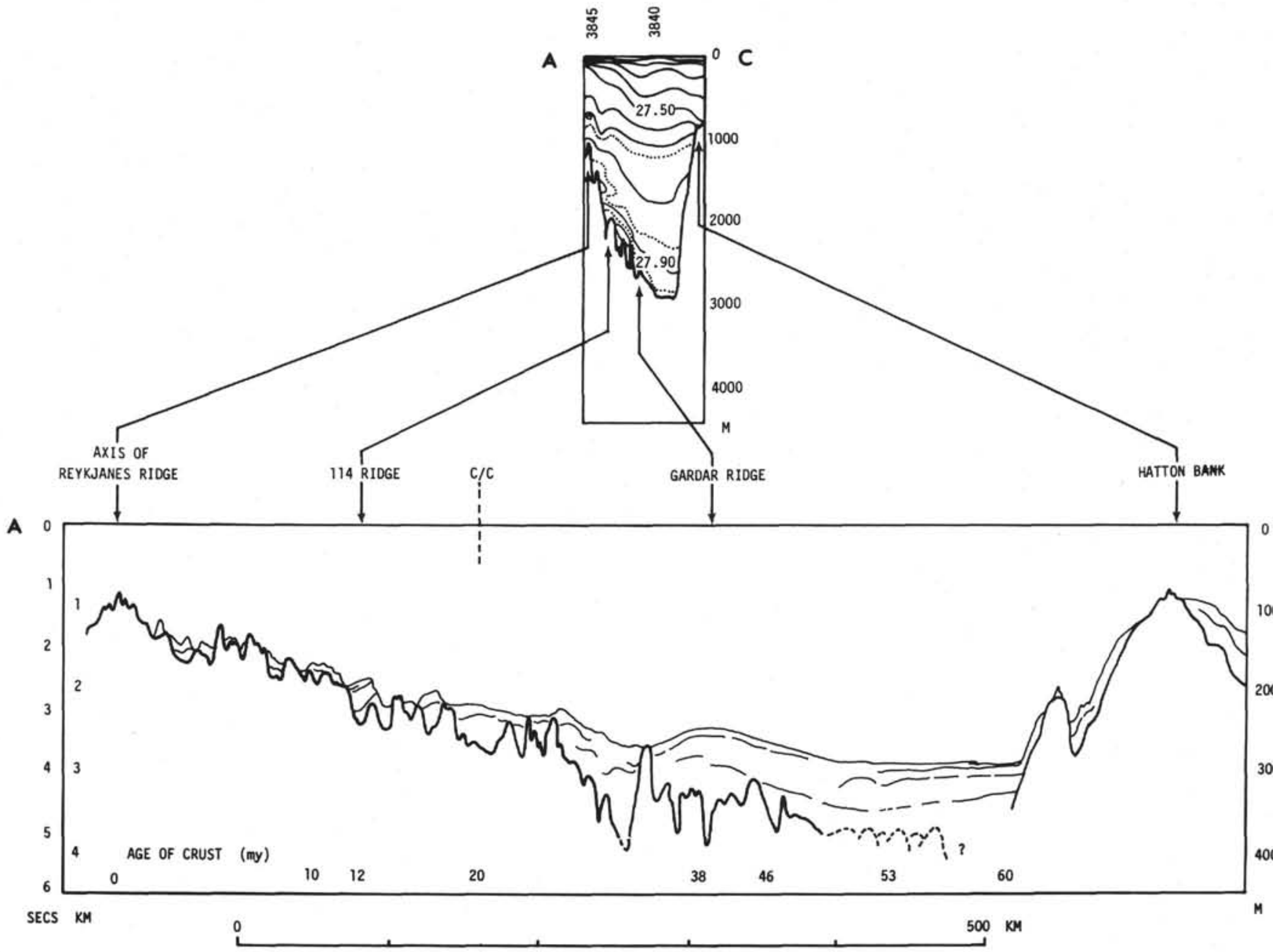

Figure 14. *Top - Potential densities from IGY hydrographic profile AC by* Discovery-*11 stations 3837-3846 across Iceland Basin. Bottom - Interpreted seismic reflection profile AB across Iceland Basin from* Vema-*23 and 27 and* Discovery-*29 data.*

The sediments sampled in Hole 114 were predominantly clays and silts with relatively little carbonate (between 5 and 50 per cent). The bulk was terrigenous material containing abundant volcanic products. Much of this may have been derived from the finer fraction of volcanic material deposited on the continental shelf and slope south of Iceland. We know from the sediments recovered at Hole 115, that turbidity currents originate on this slope carrying the coarser material into the deep part of the Iceland Basin. Two large canyons in the rise are probably cut by turbidity currents. The finer fractures may get incorporated into the westerly going bottom currents and be deposited on the flanks of the Reykjanes Ridge. Seismic profiles south of Iceland show considerable accumulations of sediment which may have been redistributed in this way.

REFERENCES

Avery, O. E., Vogt, P. R. and Higgs, R. H., 1969. Morphology, magnetic anomalies and evolution of the Northeast Atlantic and Labrador Sea. Part II, Magnetic anomalies (abstract). *Trans. Am. Geophys. Union.* **50**, 184.

Benson, R. N., 1966. *Recent Radiolaria from the Gulf of California*. Unpublished Ph. D. dissertation, University of Minnesota, Minneapolis.

De Boer, J., Schilling, J-G. and Krause, D. C., 1969. Magnetic polarity of pillow basalts from Reykjanes Ridge. *Science.* **166**, 996.

De Boer, J., Schilling, J-G. and Krause, D. C., 1970. Reykjanes Ridge – implication of magnetic properities of dredged rock. *Earth and Planet. Sci. Letters.* **9**, 55.

Ewing, J. and Ewing, M., 1967. Sediment distribution on the mid-ocean ridges with respect to spreading of the sea-floor. *Science.* **156**, 1590.

Fuglister, F. C., 1960. *Atlantic Ocean Atlas of Temperature and Salinity Profiles and Data from the International Geophysical Year of 1957-1958*. Woods Hole (Woods Hole Oceanographic Institution), 209 pp.

Godby, E. A., Hood, P. J. and Bower, M. E., 1968. Aeromagnetic profiles across the Reykjanes Ridge Southwest of Iceland. *J. Geophys. Res.* **73**, 7637.

Heirtzler, J. R., Dickson, G. O., Herron, E. M., Pitman III, W. C. and Le Pichon, X., 1968. Marine magnetic anomalies, geomagnetic field reversals and motions of the ocean floor and continents. *J. Geophys. Res.* **73**, 2119.

Heirtzler, J. R., Le Pichon, X. and Baron, J. G., 1966. Magnetic anomalies over the Reykjanes Ridge. *Deep-Sea Res.* **13**, 427.

Johnson, G. L. and Schneider, E. D., 1969. Depositional ridges in the North Atlantic *Earth and Planet Sci. Letters.* **6**, 416.

Jones, E. J. W., Ewing, M., Ewing, J. I. and Eittreim, S. L., 1970. Influences of Norwegian Sea overflow water on sedimentation in the Northern North Atlantic and Labrador Sea. *J. Geophys. Res.* **75**, 1655.

Krause, D. C. and Schilling, J-G., 1969. Dredged basalt from the Reykjanes Ridge, North Atlantic. *Nature.* **224**, 791.

Lee, A. J. and Ellett, D., 1965. On the contribution of overflow water from the Norwegian Sea to the hydrographic structure of the North Atlantic Ocean. *Deep-Sea Res.* **12**, 129.

Pitman, W. C. and Talwani, M., (in press). Sea floor spreading in the North Atlantic. *Bull. Geol. Soc. Am.*

Talwani, M., Windisch, C. C. and Langseth, M. G., 1971. Reykjanes Ridge Crest: a detailed geophysical study. *J. Geophys. Res.* **76**, 473.

Ulrich, V. J., 1960. Zur Topographic des Reykjanes-Ruckens. *Kieler Meeresforschungen.* **16**, 155.

Vogt, P. R., Avery, O. E., Schneider, E. D., Anderson, C. N. and Bracey, D. R. 1969. Discontinuities in sea floor spreading. *Tectonophysics.* **8**, 285.

Vogt, P., Ostenso, N. A. and Johnson, G. L., 1970. Magnetic and bathymetric data bearing on sea-floor spreading north of Iceland. *J. Geophys. Res.* **75**, 903.

Worthington, L. V. and Volkmann, G. H., 1965. The volume transport of the Norwegian Sea overflow water in the North Atlantic. *Deep-Sea Res.* **12**, 667.

Worthington, L. V. and Wright, W. R., 1970. *North Atlantic Ocean Atlas of Potential Temperature and Salinity in the Deep Water*. Woods Hole (Woods Hole Oceanographic Institution), 24 pp., 58 charts.

APPENDIX A. SHIPBOARD SMEAR SLIDE OBSERVATIONS

Site	Core	Section	Interval (cm)	Sand	Silt	Clay	Quartz	Feldspar	Pyroxene	Chlorite	Dark Mica	Light Mica	Dark Glass	Light Glass	Palagonite	Glauconite	Phosphorous	Pyrite	Authigenic Carbonate	Barite	Phillipsite	Other Zeolites	Micronodules	Other Minerals	Abundance	Estimated Carbonates	Foraminifera	Calcareous Nannofossils	Diatoms	Radiolaria	Sponge Spicules	Plant Debris	Fish Debris	Lithology and Comments
114	2	1	50		C	A	C							C		C		C						X		15	R	A	A		C			Silty clay; other minerals include hornblende and other detritals.
114	2	1	78		A	A	C	R		C						C		C						X		15	R	C	C					Silty clay; coarser than 50 cm; chlorite, phillipsite and geothite common.
114	2	2	68		A	A				C				C	C	A		C								15	C	C			C			Silty clay.
114	2	2	40		A	A				C				C	C	C		C			C					15	C	C	C		C			Silty clay; some brown goethite.
114	2	3	90		A	A	R	R		A			C	C		C		C			A			X	C		C	C	C		C			Silty clay; some goethite.
114	2	4	33		A	A				A				C	C	A		C			C					15	R	C			C			Silty clay; some goethite.
114	2	4	150	C	A	A	R	R		A				C		A		A			C					25	A	A	C		C			Slightly sandy silty clay; a few grains of goethite.
114	2	5	134	C	A	A				C			C	C		C		R	R		C					25	C	C	C		C			Sandy silty clay.
114	2	6	20		A	A	R	R		C				C		C		C								15	C	C	C		C			Silty clay; feldspar seen altering to chlorite.
114	2	6	95		A	A		R		C			C	C		C		C			C					5		C	C		C			Silty clay; sphalerite or goetite quite common.
114	3	2	113	C	A	A				R					C	C		R											C	R	Z			Siliceous ooze.
114	3	2	118		A	C	R	R		C					R			R										C	A	C	C			Clayey silt.
114	3	2	130	R	A	C				R			R	C		R		C											A	R	A			Clayey silt.
114	3	3	20		A	A				R			C	C	C	C		R						X		5					C			Silty clay; other minerals-limonite (R).
114	3	4	130		A	C		R		C			C	C		R		C				R		X		15		C						Clayey silt.
114	3	5	110	R	A	C		R		C			C		R			C			C						R	A	C		C			Sandy clayey silt.
114	3	5	132		D	C		C		R			C	C		R		C						X		20		R	A	R	R			Clayey silt; other minerals-limonite (C).
114	4	0	5		A	A		A					C	C				C			C					10		C	C		A			Silty clay.
114	4	0	5		C	A				R			C	C			C			C						25	C	C	C		C			Silty clay.
114	4	2	16		A	A				C			C	C	C	R		C			C	C				15		C	R		C			Silty clay.
114	4	3	120		C	A				R			C	C	C	R		C			C					15		C						Silty clay; limonite common.
114	4	4	40		C	A				C			C			C		C				C		X		25		R	C		C			Silty clay; other minerals-limonite (C).
114	4	4	134		C	A				C			C	C	C			C				C		X					C		R			Silty clay; other minerals-limonite (C).
114	4	4	100		C	A				C			C	C	C			C			C					15		A	A					Silty clay.
114	4	6	23		R	A		R		C			C	C	C	R		C			C					25	R	C	C	R	C			Silty clay; other minerals-limonite.
114	4	6	40		R	A				C			C	C	C	R		C						X		25	R	A						Silty clay; other minerals limonite (C).

D = Dominant, 65+%; A = Abundant, 41%-65%; C = Common, 16%-40%; R = Rare, 0%-15%.

Site	Core	Section	Interval (cm)	Sand	Silt	Clay	Quartz	Feldspar	Pyroxene	Chlorite	Dark Mica	Light Mica	Dark Glass	Light Glass	Palagonite	Glauconite	Phosphorous	Pyrite	Authigenic Carbonate	Barite	Phillipsite	Other Zeolites	Micronodules	Other Minerals	Abundance	Estimated Carbonates	Foraminifera	Calcareous Nannofossils	Diatoms	Radiolaria	Sponge Spicules	Plant Debris	Fish Debris	Lithology and Comments
114	5	0	13	C	A	C	C							C	C			C								30	C	A			C			Sandy silt; most of sand size particles are foraminifera.
114	5	1	53	A	A	C	R							C	C	A		C								45	A	C			C			Sandy silt; glauconite can be seen filling foraminifera.
114	5	2	122	C	A	A	R				R		C	C		C		C								45	A	A	R		R			Slightly sandy silty clay.
114	5	3	80	C	A	A	C						C	C		A		C								45	A	A			C			Sandy silty clay; most of sand size particles are foraminifera or glauconite pellets.
114	5	4	71	A	A	A	R				C		C	C		A		A								40	A	C			C			Sandy silt; glauconite seen filling foraminifera; mineral marked as dark mica could be a spinel (red brown isotropic).
114	5	4	72	C	A	A	C						C	C	C	C		C						X		40	C	C	C	C	C			Silty clay; common indet. yellow brown mineral (spinel?).
114	5	5	15	C	A	A							C	C	C	C		C								35	C	C	C		C			Sandy silt; most of sand is foraminifera; lot of indet. clay minerals.
114	5	5	140	C	A	A	R						C	C	C	A		C								40	A	C			C			Sandy silt.
114	5	6	98	C	A	A	R						A	A		A		A								10	R	C			C			Slightly sandy silt.
114	6	1	37		A	A	C						C	C		C		R								25	C	C			C			Silty clay.
114	6	1	39	C	D	C	R				R	R	R	R		A										15	C	C			C			Sandy silt; almost all glauconite and organic debris.
144	6	1	70		A	D	R						R	C		C										10	C	C			C			Silty clay.
114	6	4	133		C	A	C						C	C		C					R					15		C			C			Silty clay.
114	6	4	139		C	D	R						C	C		C		C								15			C		C			Slightly silty clay.
114	6	6	12		C	D						C	C			C		C									C	A			C			Slightly silty clay.
114	6	6	44		C	D	R						C	C		A										15		C			C			Slightly silty clay.
114	6	6	65		C	D							R	R		R		C				R				20		C	C		C			Slightly silty clay.
114	6	6	85		C	D								R		R		C				C				25	C	A			C			Slightly silty clay.
114	6	6	145		C	A	C	R			R		C	C				C				C				15	C	A			C			Silty clay.

APPENDIX B
Grainsize Determinations on Samples From Site 114[1]

Site	Core	Section	Interval	Percent Sand	Percent Silt	Percent Clay	Classification
114	2	2	90.0	1.9	56.4	41.7	Clayey silt
114	2	3	90.0	0.4	57.3	41.1	Clayey silt
114	2	5	118.0	4.5	57.1	38.5	Clayey silt
114	2	6	24.0	6.9	60.4	32.7	Clayey silt
114	3	2	25.0	1.0	65.5	33.5	Clayey silt
114	3	3	19.0	8.2	64.2	27.6	Clayey silt
114	3	5	29.0	5.0	67.0	28.1	Clayey silt
114	4	4	90.0	0.5	64.8	34.7	Clayey silt
114	4	5	54.0	0.6	65.2	34.2	Clayey silt
114	5	0	11.0	31.2	49.6	19.2	Sandy silt
114	5	1	54.0	37.9	43.8	18.2	Sandy silt
114	5	4	50.0	19.9	57.2	22.9	Clayey silt
114	6	6	31.0	1.4	58.7	39.9	Clayey silt

[1] Analyses carried out under the supervision of G. W. Bode and R. E. Boyce, Scripps Institution of Oceanography.

APPENDIX C
Carbon-Carbonate Content of Samples From Site 114[1]

Site	Core	Section	Top Interval	Hole Depth	Total Carbon	Organic Carbon	$CaCO_3$
114	2	2	80.0	202.3	1.7	0.2	13
114	2	3	0.0	203.0	1.7	0.1	13
114	2	5	15.0	206.1	1.4	0.2	10
114	2	6	15.0	207.6	2.5	0.1	20
114	3	2	19.0	301.8	1.1	0.2	7
114	3	3	13.0	303.1	1.6	0.3	11
114	3	5	34.0	306.3	1.9	0.3	14
114	4	2	25.0	401.8	1.2	0.2	8
114	4	4	95.0	405.5	1.0	0.2	7
114	4	5	54.0	406.5	1.6	0.0	13
114	5	0	67.0	499.2	6.0	0.2	48
114	5	1	54.0	500.5	5.5	0.2	44
114	5	4	67.0	505.2	3.3	0.2	26
114	5	6	116.0	508.7	4.2	0.1	34
114	5	6	146.0	509.0	2.4	0.3	18
114	6	6	29.0	607.8	3.2	0.3	24

[1] Analyses carried out under the supervision of G. W. Bode and R. E. Boyce, Scripps Institution of Oceanography.

APPENDIX D. LIST OF SELECTED PLANKTONIC AND BENTHONIC FORAMINIFERA AND AGE DETERMINATIONS

W. A. Berggren

Site 114

Sample 12-114-1-5, 150 cm:
PF: *Globigerina pachyderma* (abundant, dominant, sinistrally coiled), *Globigerina bulloides, Globorotalia inflata*.
BF: Sparse, including *Planulina bradii, Lenticulina* sp., *Hoeglundina elegans, Melonis pompilioides*.
Also present: Sponge spicules, diatoms, radiolarians (sparse) ice-rafted detritus.
Age: Pleistocene.

Sample 12-114-1-6, 150 cm:
All data essentially same as for preceding sample above.

Sample 12-114-1, Core Catcher:
PF: *Globigerina pachyderma* (dominant, abundant sinistral), *G. bulloides, Globorotalia inflata, G. scitula, G. crassaformis, Hastigerina siphonifera*.
BF: *Pyrgo* sp., *Eponides tenera, Planulina bradii, Lenticulina pliocaenicus, Melonis pompilioides, Hoeglundina elegans, Pyrulina angusta, Gyroidina neosoldanii, Elphidium* sp.
Also present: Echinoid spines, ostracods, ice-rafted detritus including basalt fragments.
Age: Pleistocene (glacial).

Sample 12-114-2-0, Bottom:
PF: *Globigerina pachyderma* (dextral), *G. bulloides, G. inflata, G. scitula*.
BF: Sparse, including *Melonis pompilioides*.
Also present: Sponge spicules, diatoms, echinoid spines.
Age: Pleistocene (?interglacial).

Sample 12-114-2-1, 98-100 cm:
Data essentially same as for preceding sample above. This is a foraminiferal "sand" intercalated within a soft olive-gray terrigenous clay-silt.
Age: Pleistocene (?interglacial).

Sample 12-114-2-2, 143-145 cm:
Data essentially same as preceding above. Lithology is a soft olive-gray terrigenous clay-silt with foraminiferal remains in matrix.
Age: Pleistocene (?interglacial).

Sample 12-114-2-3, 143-145 cm:
See Sample 12-114-2-1, 98-100 cm above.
Age: Pleistocene (?interglacial).

Sample 12-114-2-4, 142-145 cm:
See preceding sample above.
Age: Pleistocene (?interglacial).

Sample 12-114-2-5, 142-145 cm:
See preceding sample above.
Age: Pleistocene (?interglacial).

Sample 12-114-2, Core Catcher:
PF: *Globigerina bulloides, G. pachyderma* (primarily dextral), *Globorotalia inflata, G. crassaformis, G. scitula*.
BF: *Quinqueloculina* sp., nodosariids, *Melonis barleeanum, Oolina* sp.
Also present: ostracods (*Echinocythereis* sp.), (?) pyritized worm holes, echinoid spines, sponge spicules, Radiolaria (rare).
Age: Pleistocene (?interglacial).

Sample 12-114-3-1, Bottom:
PF: *Globigerina atlantica, G. bulloides*.
BF: Sparse, *Cibicides* sp., *Stilostomella* sp.
Also present: Glass shards, sponge spicules, diatoms; solution effects visible in foraminiferal fauna.
Age: Late Pliocene.

Sample 12-114-3-2, 138-141 cm:
Data essentially same as for preceding sample above.
Age: Late Pliocene.

Sample 12-114-3-3, 25-28 cm:
Data essentially same as for preceding sample.
Age: Late Pliocene.

Sample 12-114-3-4, 147-150 cm:
Data essentially same as for preceding sample.
Age: Late Pliocene.

Sample 12-114-3-5, 109-112 cm:
Data essentially same as for preceding sample.
Age: Late Pliocene.

Sample 12-114-3, Core Catcher:
PF: *Globigerina atlantica, Globorotalia inflata* (rare).
BF: polymorphinids, nodosariids, *Melonis barleeanum, Quinqueloculina* sp., *Gyroidina* sp.
Also present: Volcanic ash, echinoid spines, diatoms, pyrite fragments.
Age: Late Pliocene.

Sample 12-114-4-0, 13-16 cm:
PF: *Globigerina atlantica, G. bulloides, Globorotalia scitula, Orbulina universa*.
BF: Sparse, including *i. al., Uvigerina hollicki, Pullenia* sp.
Also present: Diatoms, Radiolaria, sponge spicules, volcanic glass, pyrite.
Age: Pliocene.

Sample 12-114-4-2, 120.5-122.5 cm:
Data same as preceding sample above.

Sample 12-114-4-3, 145-147 cm:
Data same as above.

Sample 12-114-4-4, 142-144 cm:
Data same as above; planktonic and benthonic foraminiferal fauna sparse.

Sample 12-114-4-5, 143-145 cm:
Data same as above.
Age: Pliocene.

Sample 12-114-4-6, 143-145 cm:
Data same as above.
Age: Pliocene.

Sample 12-114-4, Core Catcher:
PF: *Globigerina bulloides, G. atlantica* (4 chambers, rare).
BF: *Planulina ariminensis, Cassidulina* sp.
Also present: Abundant diatoms, Radiolaria, sponge spicules, volcanic glass.
Age: Pliocene.

Sample 12-114-5, Top:
PF: Rich fauna with *Globigerina atlantica, Globigerina bulloides, Globigerina* sp., *Orbulina universa, Floborotalia crassaformis, G. inflata*.
BF: *Sigmoilopsis schlumbergeri, Pyrulina* sp., *Melonis pompilioides, Uvigerina* sp., *Trifarina* sp., *Bulimina* sp., *Pleurostomella* sp.
Also present: Abundant ?glauconite (filling in foraminiferal chambers), echinoid spines, sponge spicules.
Age: Pliocene.

The following samples in this core contain essentially the same fauna as listed above.

Sample 12-114-5-1, 142-145 cm
Sample 12-114-5-2, 128-131 cm
Sample 12-114-5-3, 145-148 cm
Sample 12-114-5-4, 138-141 cm
Sample 12-114-5-5, 20-22 cm
Sample 12-114-5-5, 65-67 cm
Sample 12-114-5-5, 98-100 cm
Sample 12-114-5-5, 119-121 cm
Sample 12-114-5-5, 141-143 cm
Sample 12-114-5-6, 4-6 cm
Sample 12-114-5-6, 99-100 cm

Note: The abundant ?glauconite occurs above this level; the samples below contain volcanic ash and glass.

Sample 12-114-5-6, 129-131 cm

Sample 12-114-5, Core Catcher:
PF: *Globigerina atlantica, G. bulloides, G.* sp., *Globorotalia crassaformis, G.* cf. *miroensis*.
BF: *Uvigerina* sp., *Melonis pompilioides, Eponides tenera, Planulina ariminensis, Pyrulina* sp.
Also present: Ostracods, volcanic glass, pyrite.
Age: Pliocene.
Remarks: Core 5 is characterized almost throughout by the abundant occurrence of a green, authigenic mineral resembling glauconite. It fills the interior of foraminiferal tests in many cases. The fauna is dominated by various four-chambered "globigerinids" whose taxonomic identity is extremely difficult to determine in a consistent manner. Individuals bearing a general resemblance to *Globoquadrina dutertrei* are common as are other forms bearing a general resemblance to *Globorotalia involuta* Pezzani, *Globorotalia pseudopachyderma* Cita, Premoli, Silva and Rossi, and *Globigerina conglomerata* Schwater. All are referred here to a single species: *Globigerina atlantica*.

Sample 12-114-6-1, 30-33 cm:
PF: *Globigerina* spp.
BF: *Gyroidina* sp., *Cibicides* sp., *Uvigerina* sp.
Also present: ?Glauconite, sponge spicules, radiolarians, diatoms.
Age: Miocene-Pliocene.
The following samples contain essentially the same faunal elements:
Sample 12-114-6-3, Bottom
Sample 12-114-6-4, 134-136 cm
Sample 12-114-6-5, 138-140 cm
Sample 12-114-6-6, 76-78 cm

Sample 12-114-6, Core Catcher:
PF: *Globigerina atlantica, G.* spp.
BF: *Melonis barleeanum, M. pompilioides, Uvigerina* sp., *Eponides tenera, Gyroidina neosoldanii, Cibicides pseudoungerianus, Planulina ariminensis*.
Also present: ?Glauconite, volcanic ash and glass, pyrite, Radiolaria, sponge spicules.
Age: Miocene-Pliocene.
Only water samples were obtained from Cores 7 and 8 and these contain mixed (contaminated) assemblages of planktonic foraminifera.

APPENDIX E. COCCOLITH SPECIES AND STRATIGRAPHIC ASSIGNMENT OF SITE 114

David Bukry

Hole 114

Lower Pleistocene
(*Coccolithus doronicoides* Zone)

12-114-1-5, 81 cm; depth 107 m:
Cyclococcolithina leptopora, Discolithina sp. cf. *D. japonica, Emiliania annula, Gephyrocapsa caribbeanica, Helicopontosphaera kamptneri*

Upper Pliocene or Lower Pleistocene
(Transitional)

12-114-2-6, 128-130 cm: depth 209 m:
Coccolithus pelagicus [abundant], *Cyclococcolithina leptopora, C. macintyrei, Discolithina* sp., *Helicopontosphaera sellii* [abundant].

12-114-3-5, 103-104 cm; depth 305m:
Coccolithus doronicoides, C. pelagicus, Coccolithus sp. [tiny], *Cyclococcolithina leptopora, C. macintyrei, Discolithina* sp. cf. *D. japonica, D. multipora, Helicopontosphaera kamptneri, H. sellii, Scyphosphaera* sp. . Reworked Oligocene taxon: *Chiasmolithus altus*.

HOLE 114

CORE 1

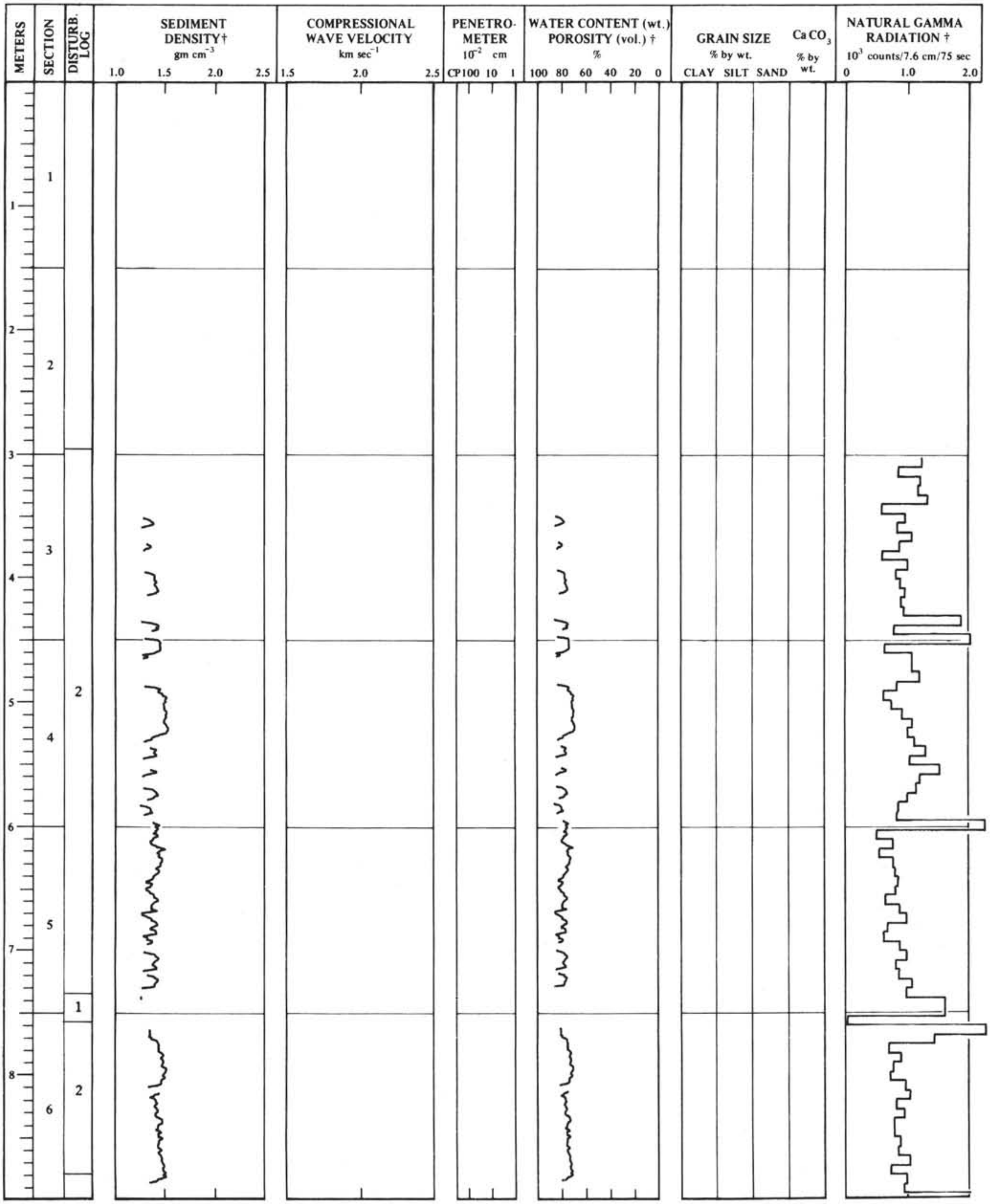

†Adjusted data, see Chapter 2

HOLE 114 100 TO 109 m

CORE 1

METERS	SECTION	LITHOL.	SAMPLES	LITHOLOGY	DIAGNOSTIC FOSSILS	BIO-STRAT.	TIME STRAT.
0–1.5	1	SECTIONS NOT OPENED		Very soft, sloppy olive gray (5Y4/2) clay. Entire core very much disturbed.		*Pseudoemiliania lacunosa*	PLEISTOCENE
1.5–3	2	EMPTY					
3–4.5	3	SECTION NOT OPENED					
4.5–6	4						
6–7.5	5		N,F		Flora: *Gephyrocapsa aperta, Syracosphaera* sp., *Pseudoemiliania lacunosa, Pontosphaera discopora, Helicopontosphaera kamptneri, (Coccolithus pelagicus)** Fauna: *Globigerina pachyderma, G. bulloides, Globorotalia inflata*		
7.5–9	6		F N		Fauna similar to above. Flora similar to above*. Radiolarians common. *Theocalyptra davisiana, Actihomma* spp., *A. antarcticum, A. medianum, Spongopyle osculosa, Spongotrochus* sp. cf. *S. glacialis, Stylodictya validispina, Spongodiscus*. spp., *Ommatodiscus* spp.		
	CC		R N F		Flora similar to above.* *G. pachyderma, G. bulloides, G. inflata, G. scitula, G. crassaformis, H. siphonifera*		

**Coccolithus pelagicus* is very rare. Some reworked Late Cretaceous coccoliths occur.

HOLE 114

CORE 2

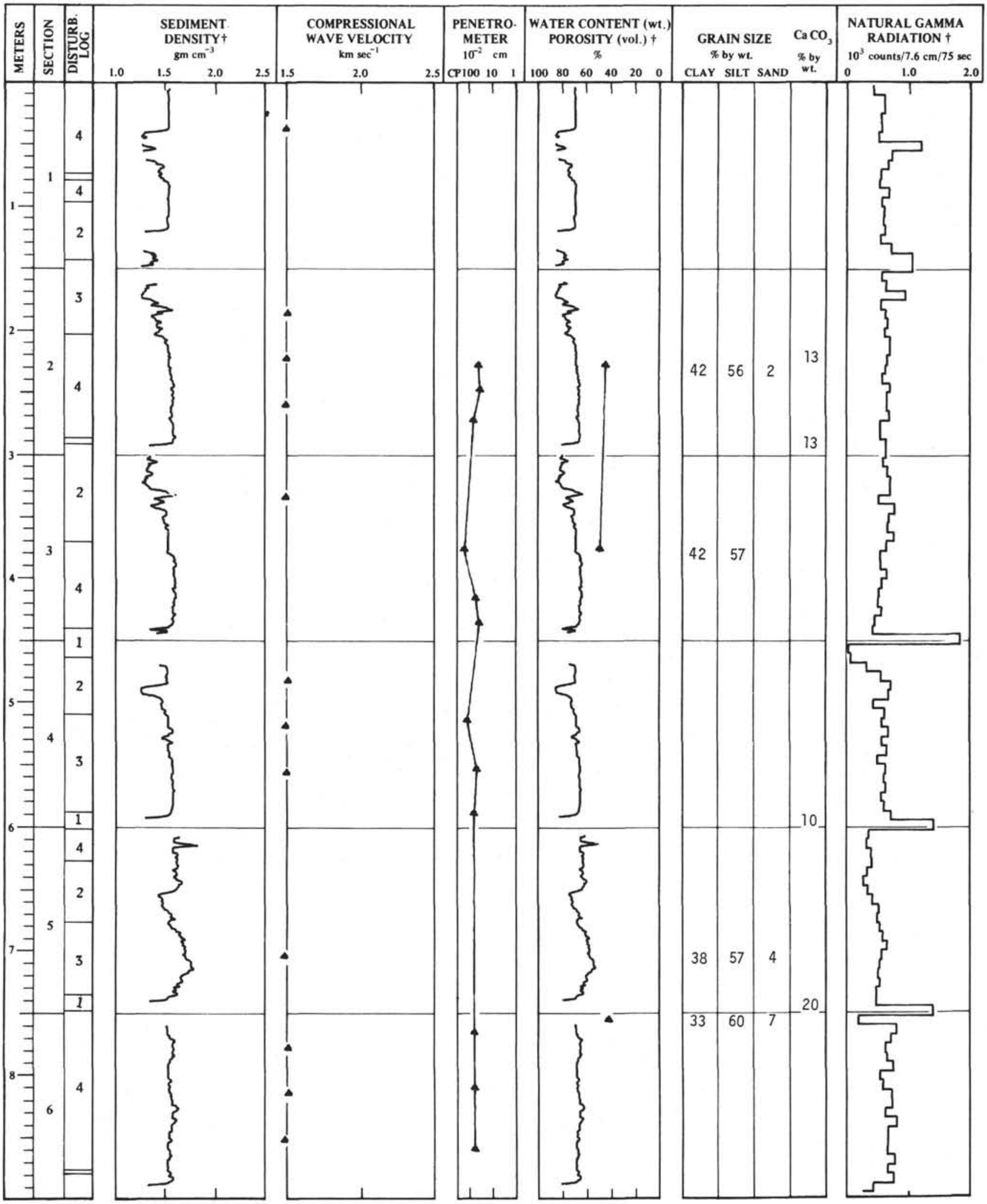

†Adjusted data, see Chapter 2

HOLE 114 200 TO 209 m

CORE 2

METERS	SECTION	LITHOL.	SAMPLES	LITHOLOGY	DIAGNOSTIC FOSSILS	BIO-STRAT.	TIME STRAT.
0–1.5	1		N,F / N / F	5Y2/1. Alternating layers of firm and soupy olive black clay. Quartz and clay pebbles found at the bottom of Section 1. Section 1 is disturbed	Flora: *Coccolithus pelagicus, Helicopontosphaera kamptneri, H. sellii, Rhabdosphaera clavigera, Syracosphaera* sp. *Pontosphaera discopora, Pseudoemiliania lacunosa* Flora similar to above plus *Cyclococcolithus leptoporus, C. macintyrei* Fauna: *Globigerina pachyderma, G. bulloides, Globorotalia inflata, G. scitula*	*Pseudoemiliania Lacunosa*	PLEISTOCENE
1.5–3	2		N / F	5G4/1 to 5G2/1. Soft to soupy greenish black clay. Sediment is disturbed. Coarse fraction is almost entirely foraminifera and sponge spicules. Some well rounded quartz grains.	Flora similar to above. Fauna similar to above.		
3–4.5	3		N / F	5G2/1. Dry, firm, greenish-black silty clay, slightly mottled dark gray. Thick shell fragments found at 138-147cm in Section 3.	Flora similar to above.		
4.5–6	4		N / F	Dark, greenish-gray silty clay. Some disturbance apparent. Foram sand.	Fauna similar to above. Flora similar to above.		
6–7.5	5	EMPTY	N / F	5GY2/1 to 5GY4/1. Hard lumps of firm clay in a silty, foram rich sand matrix passing down into slightly mottled greenish gray clay. Some pyrite seen in coarse fraction. Foram sand	Fauna similar to above. Flora similar to above. Fauna similar to above.		
7.5–9	6	EMPTY	N	Foram sand	Flora similar to above. Radiolarians rare. Same as in core catcher of core 10.		
	CC		R / N / F	Silty clay	Flora similar to above. Fauna: *Globigerina bulloides, G. pachyderma, Globorotalia inflata, G. crassaformis, G. scitula.*		

X-ray minerology (bulk)	
Calcite	23.7
Qtz.	6.1
Plag.	24.3
Mica	6.9
Chlorite	3.6
Mont.	3.0
Augite	32.2
Amorph.	76.3

HOLE 114

CORE 3

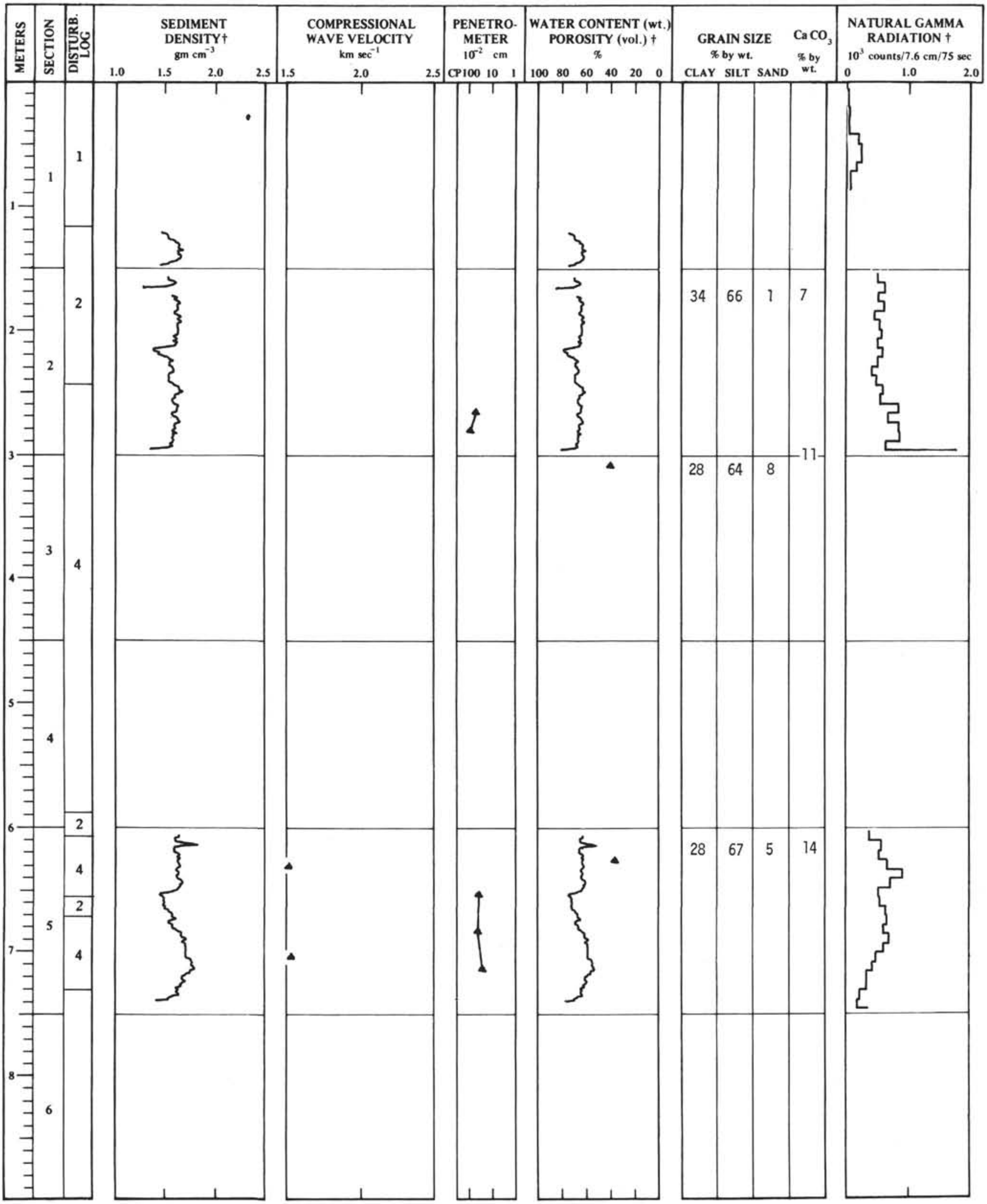

†Adjusted data, see Chapter 2

HOLE 114 300 **TO** 309 **m**

CORE 3

METERS	SECTION	LITHOL.	SAMPLES	LITHOLOGY	DIAGNOSTIC FOSSILS	BIO-STRAT.	TIME STRAT.
0–1.5	1	SECTION NOT OPENED	N,F	Very soupy greenish gray clay.	Flora: *Coccolithus pelagicus, Cyclococcolithus leptoporus, Discoaster* sp. *Pontosphaera scutellum, P. discopora, Reticulofenestra pseudoumbilica ?, Helicopontosphaera kamptneri, H. sellii.* Fauna: *Globigerina atlantica, G. bulloides*		
1.5–3	2	EMPTY / EMPTY / EMPTY	N; F	5Y4/1; 5Y4/2	Flora similar to above. Fauna similar to above.		
3–4.5	3	EMPTY	N,F	5GY4/1. Dark gray silty clay and dark gray clay pebbles alternating with dark gray smooth clay in a generally disturbed and watery matrix. Coarse fraction contains many small forams, mica flakes, mineral grains and sponge spicules.	Flora similar to above. Fauna similar to above.		
4.5–6	4		N; F		Flora similar to above. Fauna similar to above.		
6–7.5	5	EMPTY	N; F	5Y4/1; 5Y3/1. Upper 20cm of Section 5 contains pyrite nodules. Lower 25cm of Section 5 consists of hard laminated, friable, clayey mudstone.	Flora similar to above, plus *Pseudoemiliania lacunosa.* Fauna similar to above.		PLIOCENE
	CC		R, N, F	**Core Catcher:** Clay	**Core Catcher:** Radiolarians abundant: *Spongaster* sp. cf. *S. tetras* plus assemblage of core catcher of core 1. Flora similar to above. Fauna: *Globigerina atlantica, Globorotalia inflata*		

X-ray mineralogy (bulk)	
Calcite	30.2
Qtz.	2.1
Plag.	22.2
Kaol.	1.0
Pyrite	1.8
Augite	42.4
Amorph.	81.8

HOLE 114

CORE 4

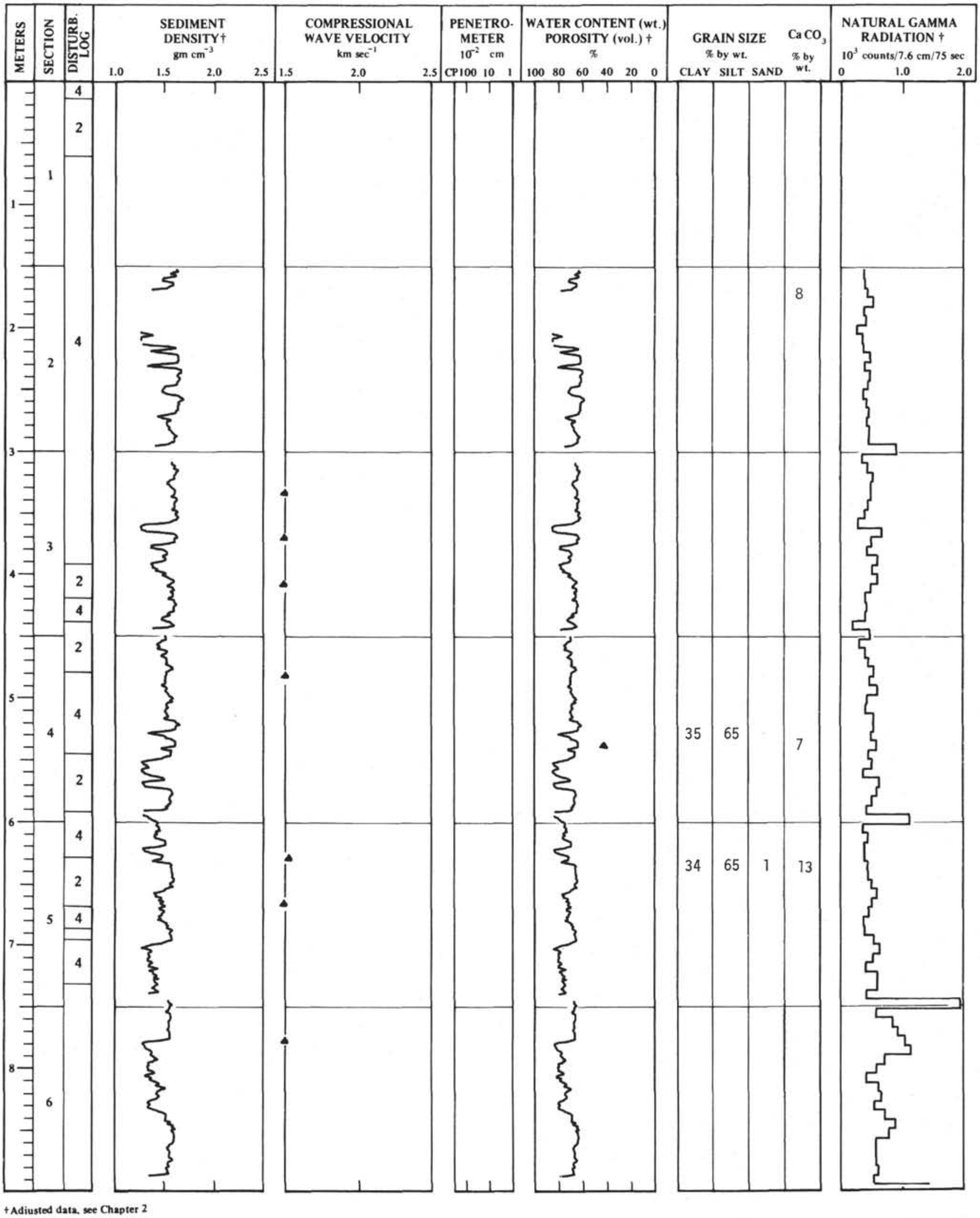

†Adjusted data, see Chapter 2

HOLE 114 400 TO 409 m

CORE 4

METERS	SECTION	LITHOL.	SAMPLES	LITHOLOGY	DIAGNOSTIC FOSSILS	BIO-STRAT.	TIME STRAT.
0–1.5	1	SECTION NOT OPENED	F, N	Very soft sediment.	Fauna: *Globigerina atlantica, G. bulloides, Globorotalia inflata, Orbulina universa* Flora: *Coccolithus pelagicus, Cyclococcolithus leptoporus, Pseudoemiliania lacunosa, Reticulofenestra pseudoumbilica, Helicopontosphaera kamptneri, H. sellii.*	*Reticulofenestra pseudoumbilica?*	PLIOCENE
1.5–3	2	EMPTY (bottom)	N, F	5Y2/1; 5Y4/1	Flora similar to above. Fauna as above.		
3–4.5	3		N, F	5Y2/1 Alternating layers of gray clayey mudstone, sticky plastic clay and soupy clay. Shell fragments and mineralized pockets scattered through Section 3. Coarse fraction shows many indeterminate recrystallized lumps, pyritized worm burrows, forams, sponge spicules, small mica grains and pyrite lumps.	Flora similar to above. Fauna similar to above.		
4.5–6	4	EMPTY	N, F	X-ray mineralogy (bulk): Calcite 28.8; Qtz 1.4; Plag. 35.2; Pyrite 2.0; Augite 32.4; Amorph. 78.1	Flora similar to above. Fauna similar to above.		
6–7.5	5	EMPTY; EMPTY; EMPTY	N, F	5Y3/1	Flora similar to above. Fauna similar to above.		
7.5–9	6		N, F	5GY3/1	Flora similar to above. Radiolarians abundant. *Ommatodiscus* spp., *Eucyrtidium calvertense, Euchitonia* sp., *Spongodiscus biconcavu, Theocalyptra davisiana, Druppatractus irregularis, Stylodictya validispina.*		
	CC		R, N, F		Flora similar to above. Fauna: *Globigerina atlantica, G. bulloides*		

HOLE 114

CORE 5

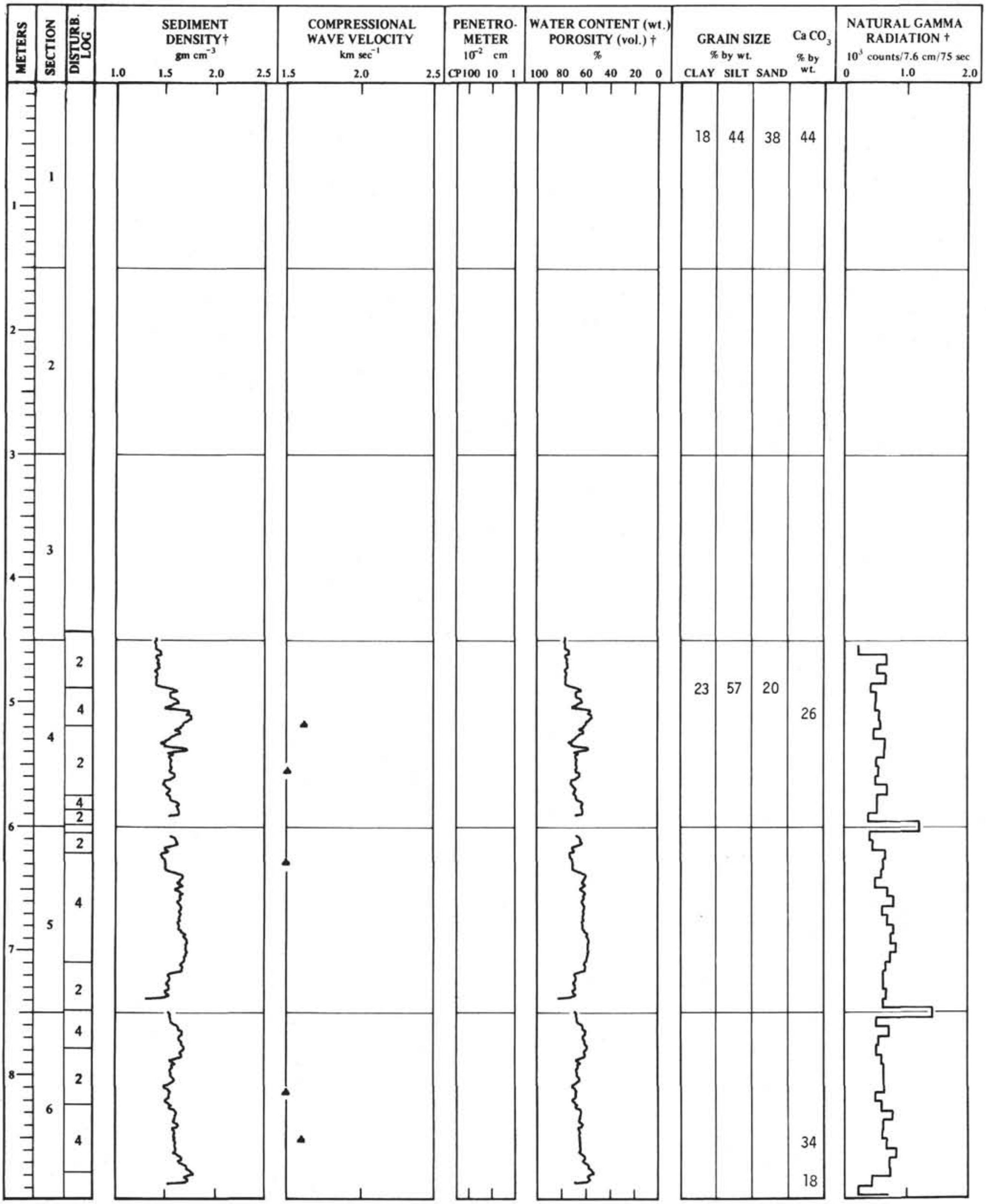

†Adjusted data, see Chapter 2

HOLE 114 500 **TO** 509 **m**

CORE 5

METERS	SECTION	LITHOL.	SAMPLES	LITHOLOGY	DIAGNOSTIC FOSSILS	BIO-STRAT.	TIME STRAT.
0–1.5	1	EMPTY G WATERY G WATERY G G G G G	N,F N F	Hard, greenish-gray glauconite-rich sandy silt alternating with watery sediment. Coarse fraction shows a mixture of glauconitized forams, fresh or partially pyritized forams and sponge spicules. X-ray mineralogy (bulk) Calcite 75.0 Qtz. 1.2 Plag. 11.2 Augite 12.5 Amorphous 69.8	Flora: *Coccolithus pelagicus, Cyclococcolithus leptoporus, C. macintyrei, Reticulofenestra pseudoumbilica Pontosphaera discopora, Helicopontosphaera kamptneri, H. sellii, Syracosphaera* sp. *Scyphosphaera* sp. Fauna: *Globigerina atlantica, G. bulloides, Orbulina universa, Globorotalia crassaformis, G. inflata* Fauna similar to above.		PLIOCENE
1.5–3	2	WATERY G G G EMPTY	N F	5GY6/1 Sticky, glauconitic silty clay.	Flora similar to above. Fauna similar to above.		
3–4.5	3	G G G G G G G G G G G G G G G G G	N F	Disturbed, watery, glauconitic, greenish gray clayey silt.	Flora similar to above. Fauna similar to above.		
4.5–6	4		N F	Hard, green-gray silty clay. Watery, gray silty clay. Soft gray clay.	Flora similar to above, poorer. Fauna similar to above.		
6–7.5	5	G G G G G G G G G G G G G G G	N,F N,F N N,F N,F F	5GY4/1 Glauconitic silty sand.	Flora and fauna similar to above. Flora and fauna similar to above. Flora and fauna similar to above. Flora and fauna similar to above, plus *Discoaster variabilis, Sphenolithus* sp. Flora similar to above, plus *Discoaster brouweri, Sphenolithus* sp., *Cyclococcolithus macintyrei*		
7.5–9	6		F N N N,F N N	Gray silty clay. Fine laminations 130-140cm in Section 6. 5GY2/1 5G5/1 5Y3/1 5Y2/1	Fauna similar to above. Flora similar to above. Flora similar to above, plus *Ceratolithus* sp. Flora similar to above, plus *Discoaster brouweri, Ceratolithus* sp. Flora similar to above, plus *Discoaster variabilis, Sphenolithus abies*. Flora similar to above, poorer. Radiolarians abundant. Assemblage		
	CC		R N F		similar to 4-cc. *Stichocorys peregrina*. Flora similar to Sect. 6-128. Fauna: *Globigerina atlantica, G. bulloides, Globorotalia crassaformis*		

HOLE 114

CORE 6

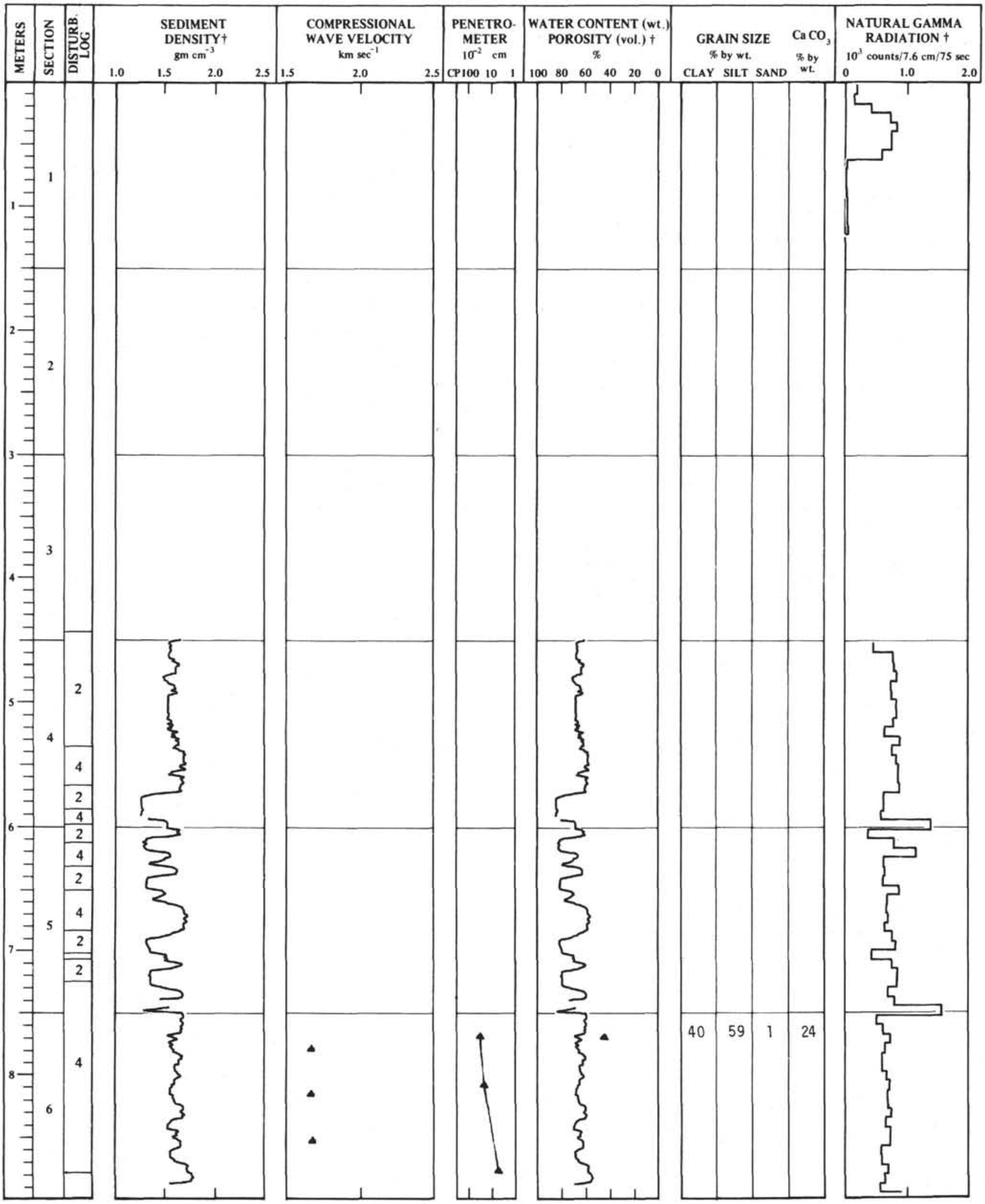

†Adjusted data, see Chapter 2

HOLE 114 600 TO 609 m

CORE 6

METERS	SECTION	LITHOL.	SAMPLES	LITHOLOGY	DIAGNOSTIC FOSSILS	BIO-STRAT.	TIME STRAT.
0–1.5	1		N,F	5GY4/1 Indurated, dark greenish gray silty sand. Faintly laminated. X-ray mineralogy (bulk) Calcite 54.2 Qtz. 3.4 Plag. 16.8 Kaol. 1.6 Mont. 2.7 Pyrite 1.8 Augite 19.4 Amorph 75.0	Flora: *Coccolithus pelagicus, Cyclococcolithus leptoporus, C. macintyrei, Pontosphaera scutellum, Sphenolithus* sp. *Ceratolithus* sp. *Helicopontosphaera kamptneri, Reticulofenestra pseudoumbilica.* Fauna: *Globigerina* spp.		
1.5–3	2	WATER					
3–4.5	3	SECTION NOT OPENED	N,F		Flora similar to above. Fauna similar to above.		
4.5–6	4	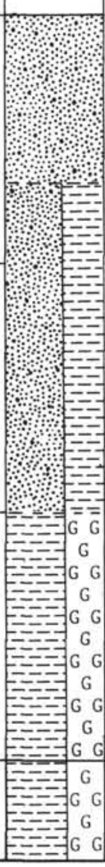	N	Dark greenish gray silty sand.	Flora similar to above, plus *Discoaster brouweri*		
6–7.5	5		N,F N F	5GY4/1 Fragments of indurated greenish gray silty sand interbedded with olive gray clay. Some mottling. Shell fragments at 76cm in Section 5. Coarse fraction shows fresh and broken, corroded forams and worm, glauconitised forams.	Flora similar to above. Fauna similar to above. Flora similar to above, plus *Discoaster* sp. Fauna similar to above.		PLIOCENE ? MIOCENE ?
7.5–9	6		N,F	5Y4/1 5YR4/1 5GY4/1 Light olive gray silty glauconitic clay. Cross-bedding at 86-90cm in Section 6; slump structure at 103-111; faint laminations at 135-150. Entire section is slightly mottled. 5Gy6/1 5Y3/2	Flora similar to above, plus *Discoaster* cf. *variabilis* Fauna similar to above.		
	CC		N F R		Flora similar to above, plus *Discoaster brouweri, D.* cf. *variabilis, Sphenolithus abies.* Fauna: *Globigerina atlantica.* Radiolarians rare. *Ommatodiscus* spp., *Stylodictya validispina, Druppatractus irregularis, Actinomma medianum, A.* spp., *Eucyrtidium calvertense.*		

HOLE 114 618 **TO** 621 **m**

CORE 7

METERS	SECTION	LITHOL.	SAMPLES	LITHOLOGY	DIAGNOSTIC FOSSILS	BIO-STRAT.	TIME STRAT.
					Indeterminate fauna. Flora: *Coccolithus pelagicus*, *Cyclococcolithus leptoporus*, *Reticulofenestra pseudoumbilica*, *Pontosphaera discopora*, *Helicopontosphaera kamptneri*, *H. sellii*, *Discoaster* cf. *D. bollii*		
	CC		F N	Core catcher sample only: Few grains of basalt and some palagonitic clay.			MIOCENE?

HOLE 114 621 **TO** 622 **m**

CORE 8

METERS	SECTION	LITHOL.	SAMPLES	LITHOLOGY	DIAGNOSTIC FOSSILS	BIO-STRAT.	TIME STRAT.
					Core water: radiolarians rare. Assemblage similar to above with *Stichocorys peregrina*.		
	CC		R N F	Core catcher sample only: Basalt cobble and some sand grains and clay pebbles.	Flora: *Coccolithus pelagicus*, *Reticulofenestra pseudoumbilica*; many small coccoliths. Indeterminate fauna.		

HOLE 114 622 **TO** 623 **m**

CORE 9

METERS	SECTION	LITHOL.	SAMPLES	LITHOLOGY	DIAGNOSTIC FOSSILS	BIO-STRAT.	TIME STRAT.
				40cm of basalt pieces			
	CC				No coccoliths. No foraminifera.		

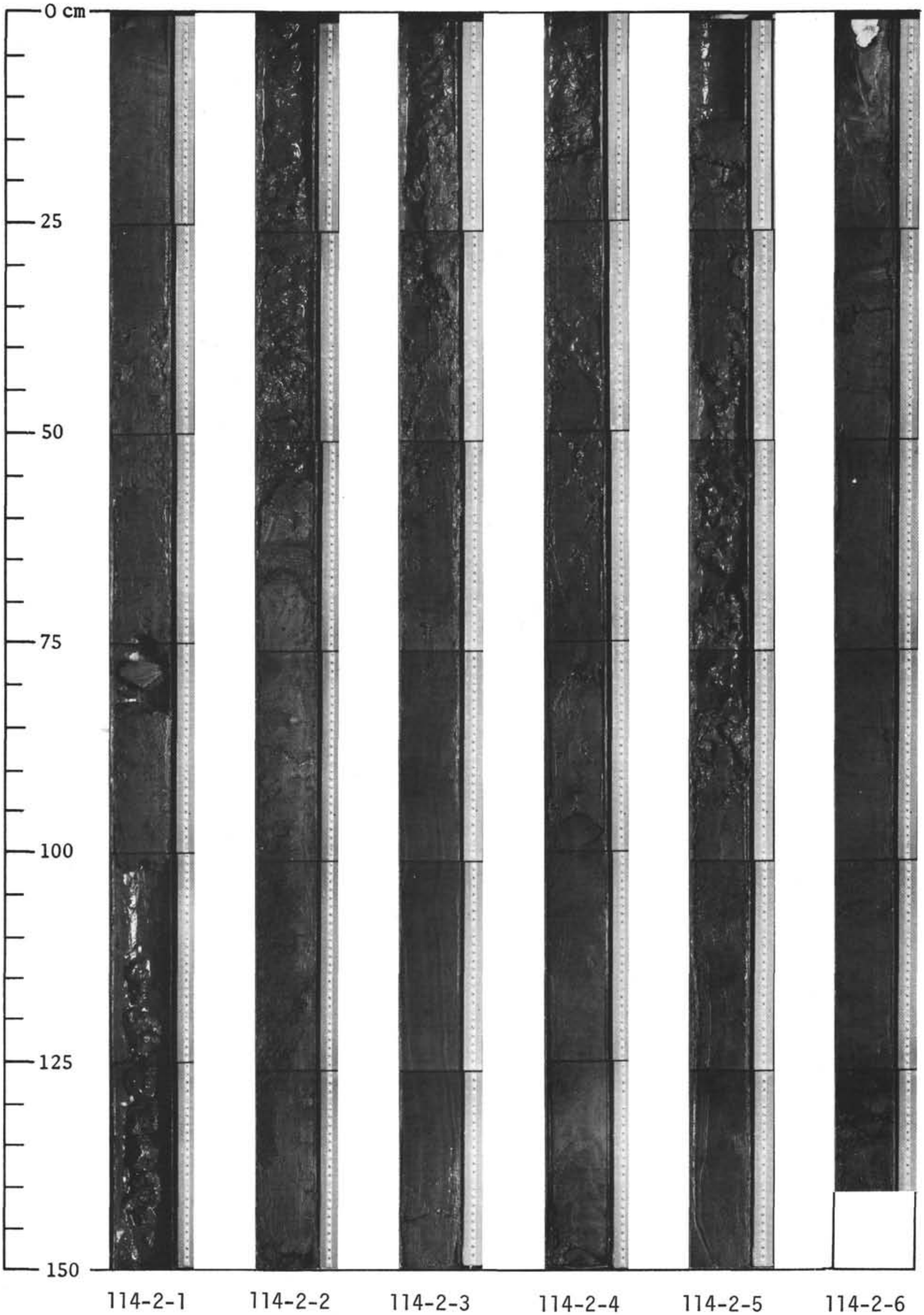
0 cm
25
50
75
100
125
150
114-2-1
114-2-2
114-2-3
114-2-4
114-2-5
114-2-6

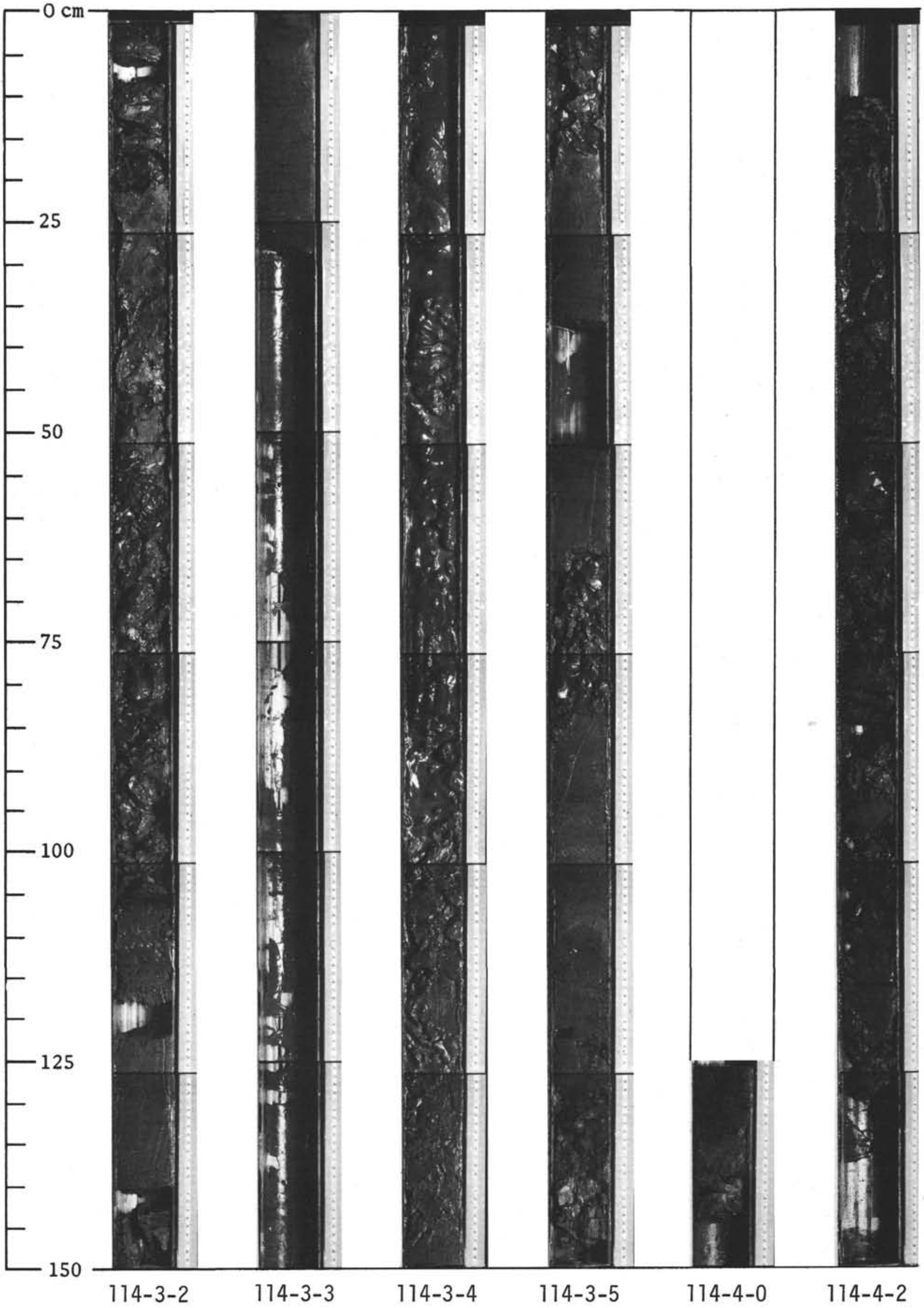
0 cm
25
50
75
100
125
150
114-3-2
114-3-3
114-3-4
114-3-5
114-4-0
114-4-2

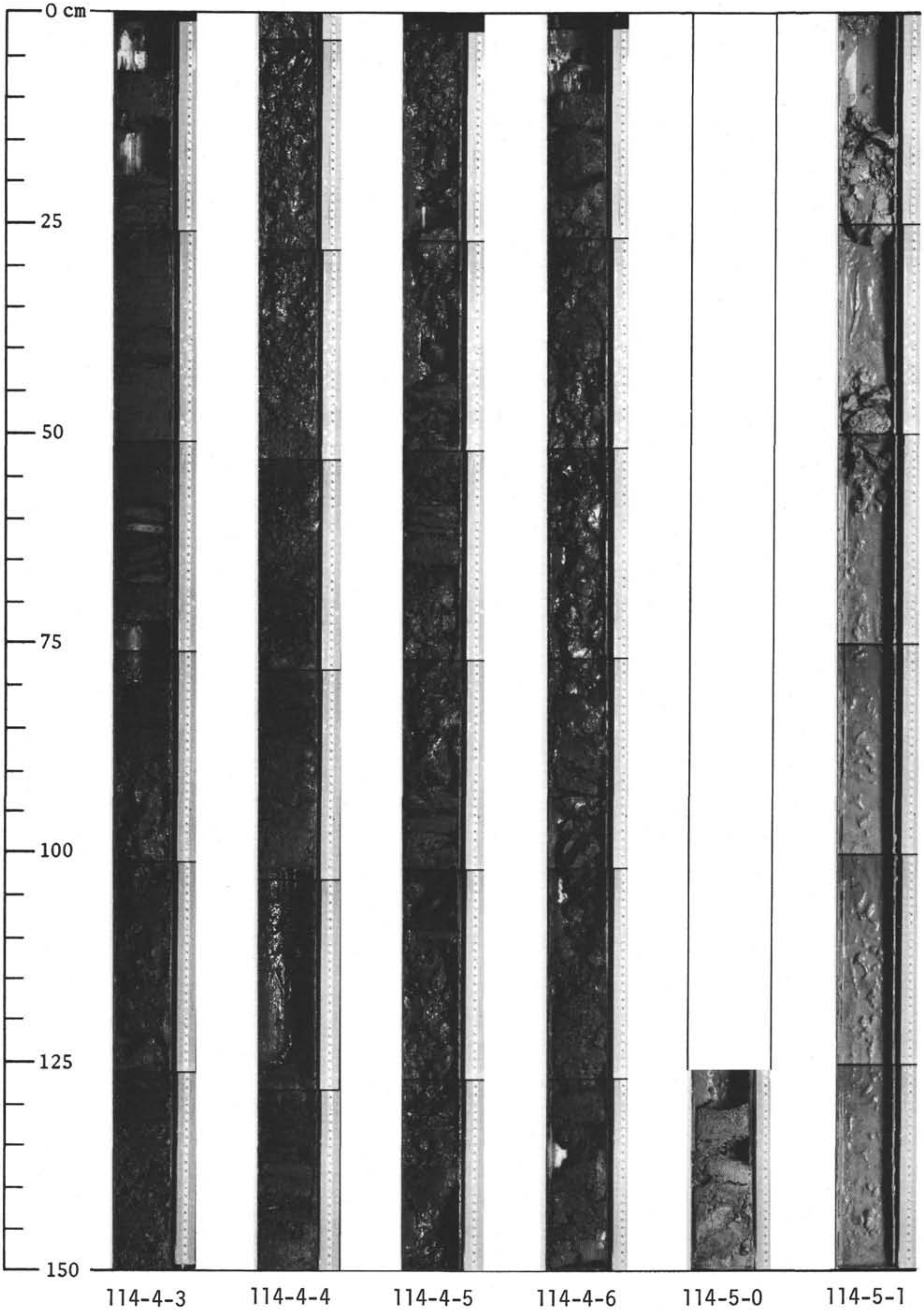

0 cm
25
50
75
100
125
150
114-4-3
114-4-4
114-4-5
114-4-6
114-5-0
114-5-1

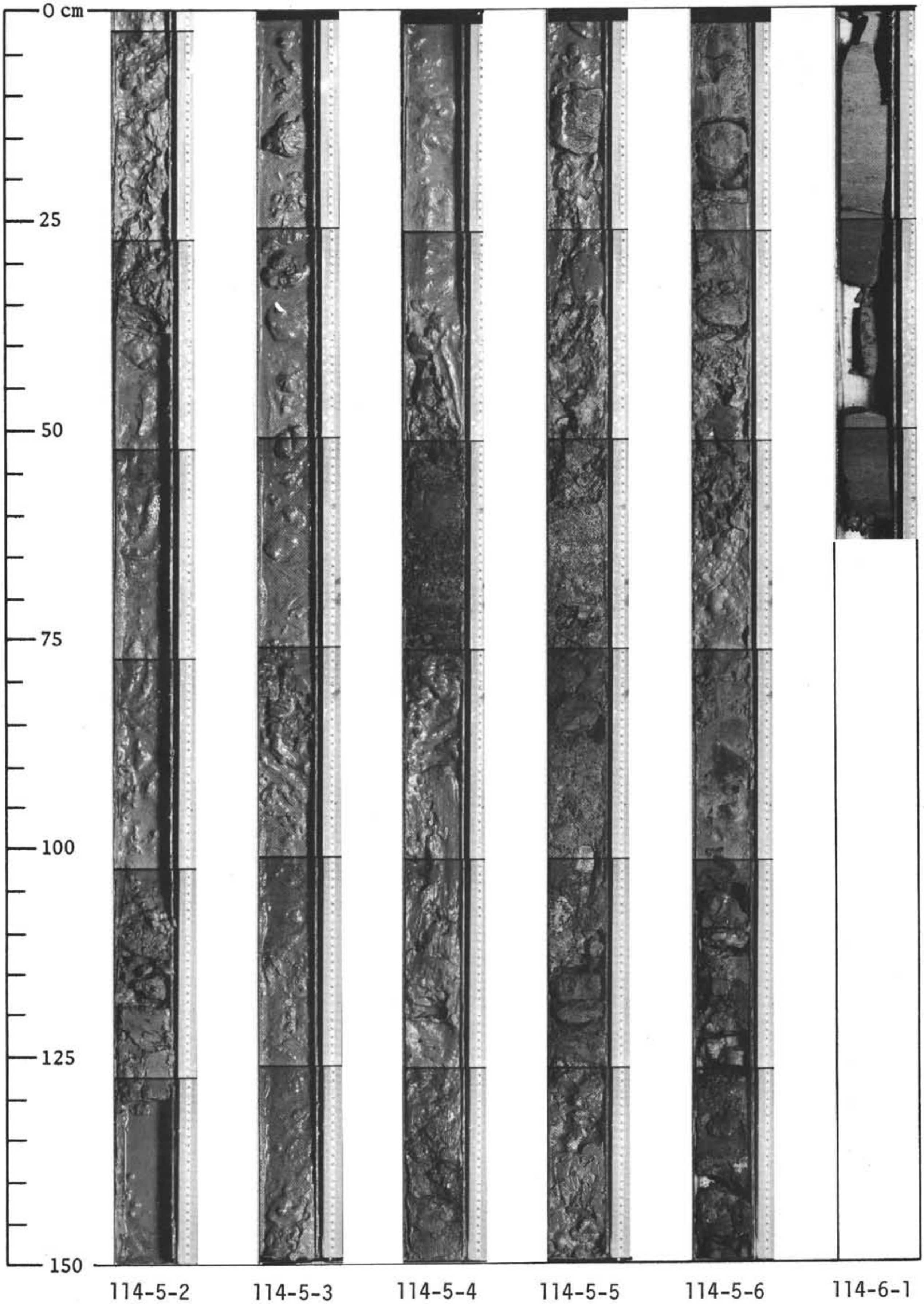
0 cm
25
50
75
100
125
150
114-5-2
114-5-3
114-5-4
114-5-5
114-5-6
114-6-1

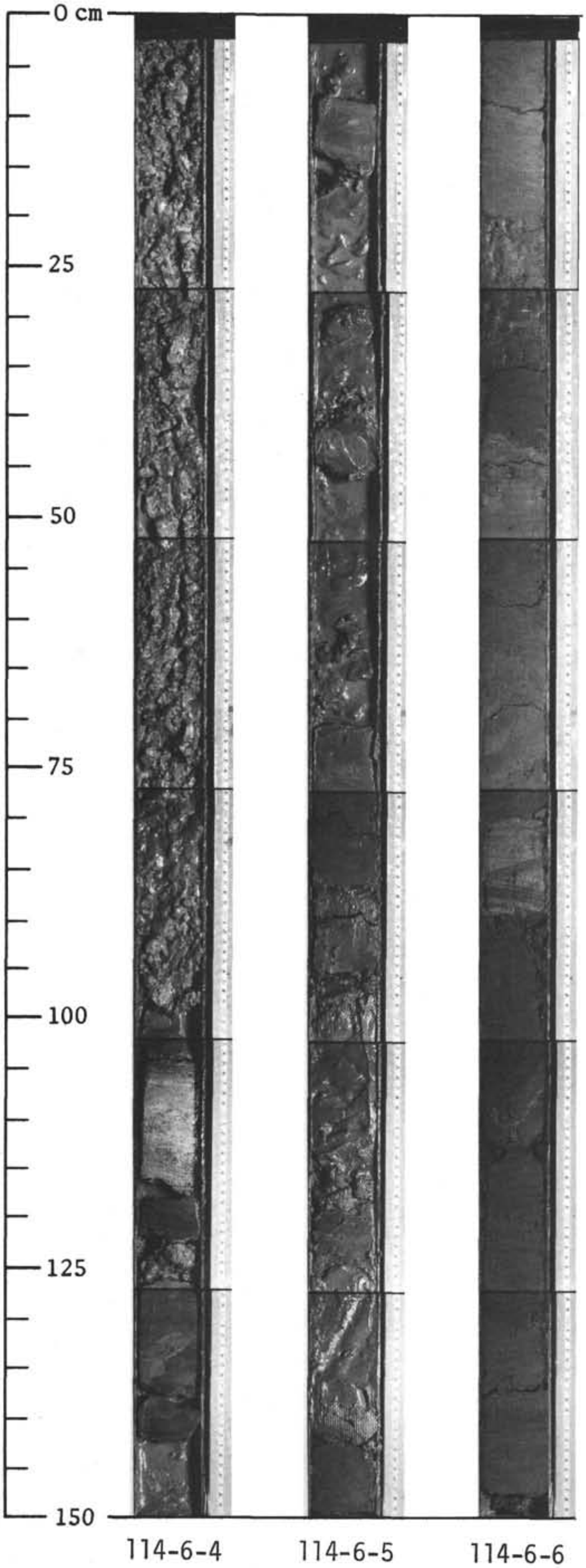
0 cm
25
50
75
100
125
150
114-6-4
114-6-5
114-6-6

SITE 114 0m TO 250m

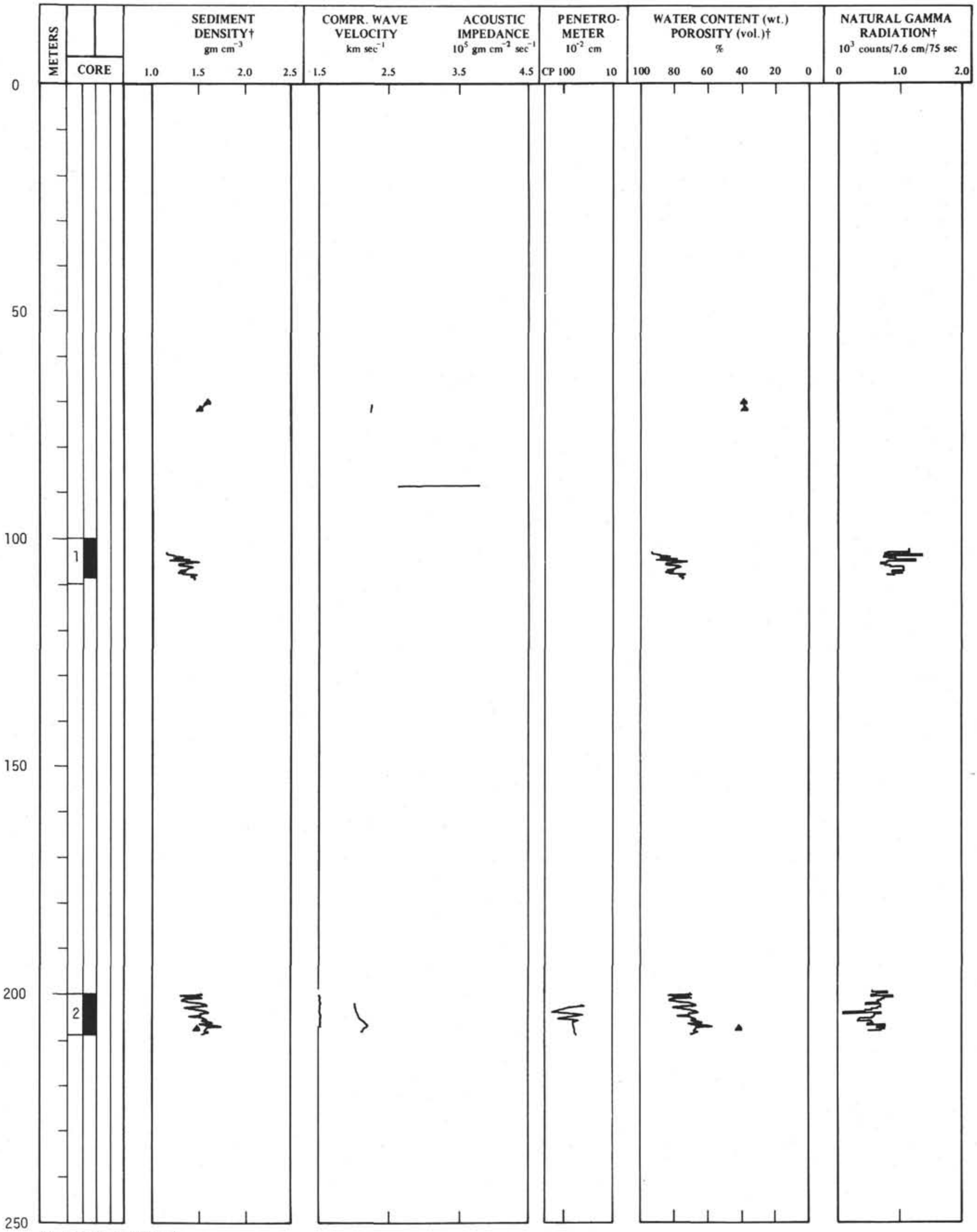

†Adjusted data, see Chapter 2

SITE 114 0 TO 250 m

METERS	CORE 114	SEISMIC REFL.	DRILL DATA	LITHOLOGY	SED. RATE cm 10^{-3}y	AGE † m. y.	TIME STRATIGRAPHIC SUBDIVISION
50							
100	1	1.65 km/sec		Soft olive gray clay.			
					12.5		PLEISTOCENE
150		0.19					
200	2			Olive gray clay with layers of foram sand.			
		0.28					
250						2	PLIOCENE

†See Chapter 2 (explanatory notes)

SITE 114 250m TO 500m

†Adjusted data, see Chapter 2

SITE 114   250 TO 500 m

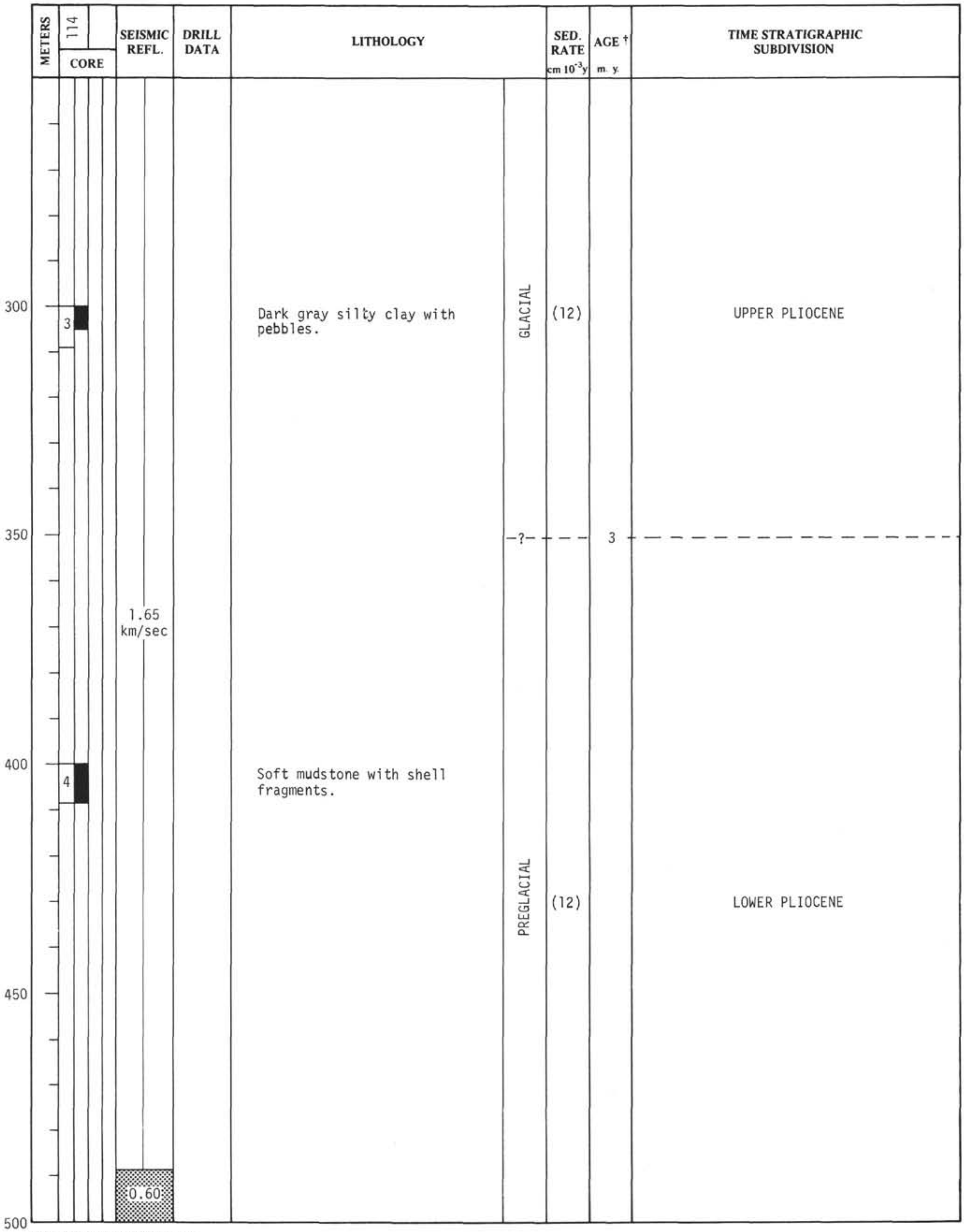

†See Chapter 2 (explanatory notes)

SITE 114 500m TO 750m

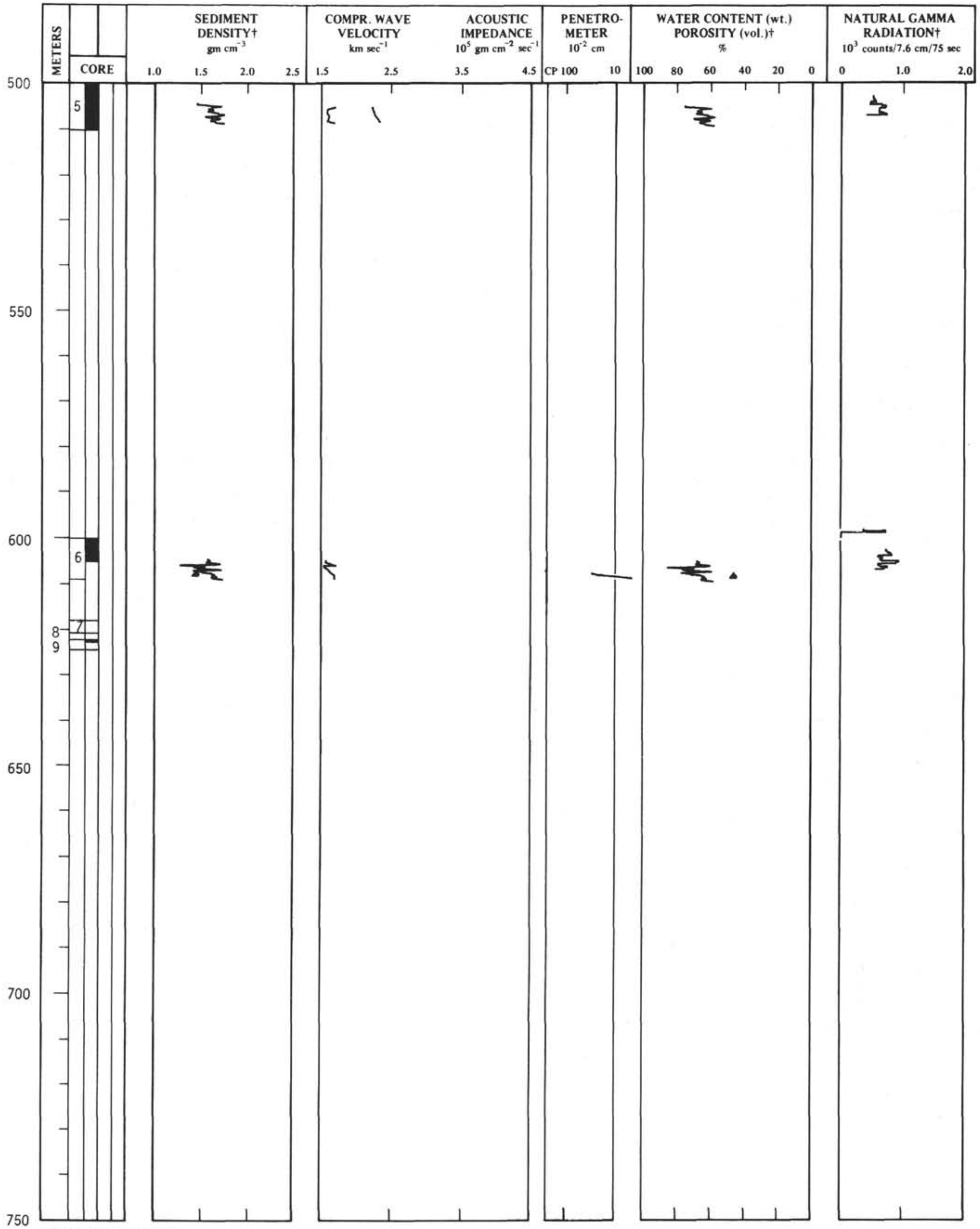

†Adjusted data, see Chapter 2

SITE 114 500 TO 750 m

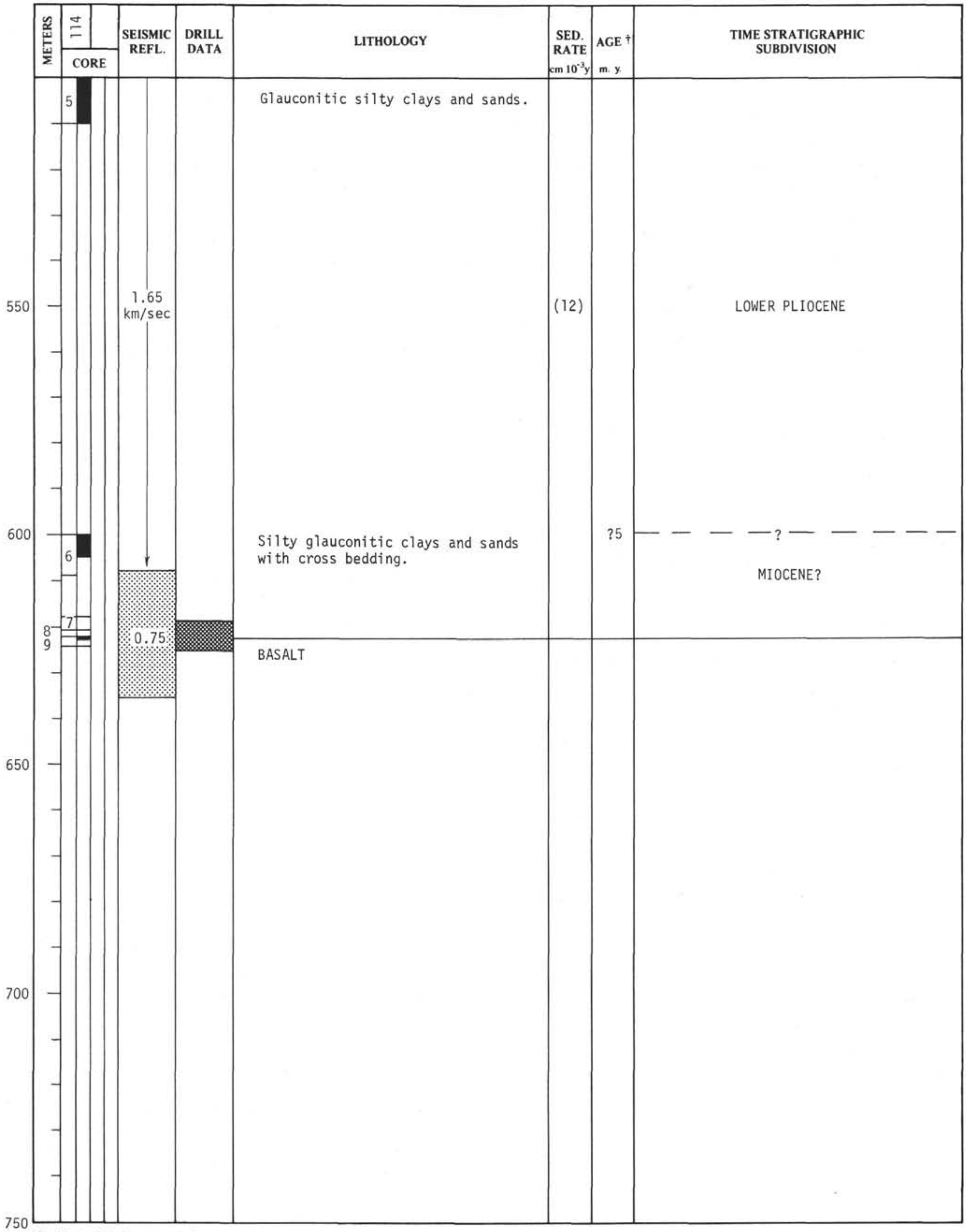

†See Chapter 2 (explanatory notes)